Spring 5-1-2015

A Study on Photodegradation and The Fate of Pyrogenic Carbon

John Thomas Howell
University of Southern Mississippi

The University of Southern Mississippi

A STUDY ON PHOTODEGRADATION AND THE FATE OF DISSOLVED PYROGENIC CARBON

by

John Thomas Howell

A Thesis
Submitted to the Graduate School
of The University of Southern Mississippi
in Partial Fulfillment of the Requirements
for the Degree of Master of Science

Approved:

Dr. Omar Harvey
Committee Chair

Dr. Franklin Heitmuller

Dr. Alan Shiller

Dr. Karen Coats
Dean of the Graduate School

May 2015

ABSTRACT

A STUDY ON PHOTODEGRADATION

AND THE FATE OF DISSOLVED PYROGENIC CARBON

by John Thomas Howell

May 2015

Accounting for all possible sources of atmospheric CO_2 is a pressing issue today due to the increasing effects of climate change. Estimates suggested that on the order of 1.3 million tons of dissolved pyrogenic carbon (*py*DOC) could be entering the northern Gulf of Mexico annually. Assessing the fate of *py*DOC in aquatic systems is crucial to understanding ecosystem impacts and potential feedback to climate change. Current research indicates that despite a generally lower susceptibility to biodegradation than their unpyrolyzed equivalents, pyrogenic carbon is not environmentally inert. While the role of microorganisms on the fate and transformation of dissolved pyrogenic carbon is well understood, very little research has been conducted to quantify contributions of abiotic processes such as photodegradation. The purpose of this study was to assess photodegradation of *py*DOC and quantify its byproducts (specifically, CO_2 evolved). The study consisted of a complimentary mix of laboratory-scale and controlled field-scale experiments with objectives of: 1) To assess the influence of solar irradiance on photodegradation of dissolved pyrogenic carbon and the nature of the degraded byproducts, 2) To assess spatiotemporal variation in photodegradation of *py*DOC in a freshwater and saltwater system, and 3) To assess the impact of salinity and depth below the water on photodegradation rates.

Natural charcoal was collected from a prescribed burn site, dissolved, and diluted to create a stock solution for testing. A sampling apparatus was made to hold the samples in a stable

position at the water surface. Samples were exposed to natural light with repeated experiments on days of varying irradiance (cloudiness). Variations in spatiotemporal influences were assessed by placing samples at different distances from shore both in a freshwater lake and in the Mississippi Sound. Experiments took place over three days with samples being collected every four hours. Following exposure, samples were tested using UV visible spectrophotometry, gas chromatography, as well as pH and electrical conductivity. Results indicated that photodegradation accounts for a 50% loss of dissolved pyrogenic carbon with the amount of photodegradation being proportional to solar irradiance. As a byproduct of photodegradation, the samples exposed to light were found to have on average more than twice as much headspace CO_2 as the dark control samples. This could be a sizable unknown source for atmospheric CO_2. Side by side tests of samples in a saline solution and samples in a distilled water solution were exposed and were found to degrade at similar rates and produce equal quantities of CO_2. Samples were also exposed at different depths below the surface of the water at 3, 6, and 12 inches. Samples at 3 inches lost 14%, while samples at 12 inches lost only 6% after one day of exposure with a total of 6.2 kW h/m^2. A curve was then constructed to predict the loss of dissolved pyrogenic carbon at a certain depth with 6.2 kW h/m^2 in one day.

ACKNOWLEDGMENTS

I would like to thank Dr. Harvey, Dr. Heitmuller, and Dr. Shiller for their edits and invaluable insight. I would like to thank the entire geology department faculty and staff, past and present, at The University of Southern Mississippi, for helping guide me to where I am today. I want to personally thank Dr. Kevin Dillon at the Southern Mississippi Gulf Coast Research Laboratory for this help and expertise with the TOC analyzer. I would also like to thank Dr. Omar Harvey for his dedication to my education and for his persistence in helping me through this process.

TABLE OF CONTENTS

ABSTRACT ii

ACKNOWLEDGMENTS iv

LIST OF ILLUSTRATIONS vi

CHAPTER

I. RATIONALE 1

II. LITERATURE REVIEW 5

III. METHODS 10

IV. INFLUENCE OF RADIATION INTENSITY ON PHOTODEGRADATION OF *py*DOC AND CO_2 PRODUCTION 12

Introduction
Results and Discussion

V. ASSESSING THE INFLUENCE OF SALINITY AND DEPTH BELOW THE SURFACE ON PHOTODEGRADATION 19

Introduction
Depth Test Results
Salinity Test Results

VI. ASSESSMENT OF *py*DOC PHOTODEGRADATION AND CO_2 IN A FRESHWATER SYSTEM 27

Introduction
Experiment #1 Results and Discussion
Experiment #2 Results and Discussion

VII. ASSESSMENT OF *py*DOC PHOTODEGRADATION AND CO_2 EMISSIONS IN A SALTWATER SYSTEM 40

Introduction
Experiment #1 Results and Discussion
Experiment #2 Results and Discussion

VIII. CONCLUSIONS 54

REFERENCES 57

LIST OF ILLUSTRATIONS

Figure

1. Study area 1

2. Map showing the average kW h/m^2/day in January for the U.S. 3

3. Map showing the average kW h/m^2/day in July for the U.S. 4

4. Graph showing the relationship of absorbance values to DOC concentrations 11

5. Samples being exposed to the sun (right) along with samples wrapping in tin foil (left) at the base of the Lake Thoreau weather station 13

6. Test #1 run at the Lake Thoreau weather station showing the light (green) and dark (red) samples compared to initial values along with the irradiance levels (blue) 16

7. Test #2 run at the Lake Thoreau weather station showing the light (green) and dark (red) samples compared to initial values along with the irradiance levels (blue) 16

8. Test #3 run at the Lake Thoreau weather station showing the light (green) and dark (red) samples compared to initial values along with the irradiance levels (blue) 17

9. Graph showing the light versus the dark values for CO_2 from test #1 17

10. Graph showing the light versus the dark values for CO_2 from test #2 18

11. Graph showing the first order kinetics from tests #1 (red), #2 (green), and #3 (blue) 18

12. Graph showing light (blue) and dark (red) samples compared to initial values at 3 inches below the surface of Lake Thoreau 21

13. Graph showing light (blue) and dark (red) samples compared to initial values at 6 inches below the surface of Lake Thoreau 21

14. Graph showing light (blue) and dark (red) samples compared to initial values at 12 inches below the surface of Lake Thoreau 22

15. Graph showing the percent loss of PyDOC with depth 22

16. Graph showing the irradiance during the depth tests 23

17. Graph showing light (blue) and dark (red) samples compared to initial values in a solution of DI water 24

18. Graph showing light (blue) and dark (red) samples compared to initial values in a solution of salt and DI water 25

19. Graph showing light (blue) and dark (red) samples compared to initial values in a solution of saltwater 25

20. Graph showing the irradiance during the salinity tests 26

21. Graph showing the first order kinetics from the salinity including the no salt test (blue), ½ salt test (green), and the salt test (red) 26

22. Picture of the sample holding apparati in Lake Thoreau 28

23. Samples attached to sample apparati with rubber bands 29

24. Arial image showing the location of the three locations used in Lake Thoreau 29

25. Graph showing the light (blue) and dark (red) samples compared to initial values in location #1 after the first Lake Thoreau three-day experiment 31

26. Graph showing the light (blue) and dark (red) samples compared to initial values in location #2 after the first Lake Thoreau three-day experiment 32

27. Graph showing the light (blue) and dark (red) samples compared to initial values in location #2 after the first Lake Thoreau three-day experiment 32

28. Graph showing the three-day total of irradiance during the first Lake Thoreau test 33

29. Graph showing the first order kinetics from the first Lake Thoreau test including location #1 (blue), location #2 (green), and location #3 (blue) 33

30. Graph showing the light (blue) and dark (red) samples compared to initial values in location #1 after the second Lake Thoreau three-day experiment 35

31. Graph showing the light (blue) and dark (red) samples compared to initial values in location #2 after the second Lake Thoreau three-day experiment 36

32. Graph showing the light (blue) and dark (red) samples compared to initial values in location #3 after the second Lake Thoreau three-day experiment 36

33. Graph showing the three-day total of irradiance during the second Lake Thoreau test 37

34. Graph showing the light versus the dark values for CO_2 after the second Lake Thoreau three-day experiment at location #1 37

35. Graph showing the light versus the dark values for CO_2 after the second Lake Thoreau three-day experiment at location #2 38

36. Graph showing the light versus the dark values for CO_2 after the second Lake Thoreau three-day experiment at location #3 38

37. Graph showing the first order kinetics from the second Lake Thoreau test including location #1 (blue), location #2 (green), and location #3 (blue) 39

38. Picture showing the location of the experiments in the Mississippi Sound 41

39. Arial image showing the area of the three locations used during testing 42

40. Graph showing the light (blue) and dark (red) samples compared to initial values in location #1 after the first Mississippi Sound three-day experiment 44

41. Graph showing the light (blue) and dark (red) samples compared to initial values in location #2 after the first Mississippi Sound three-day experiment 44

42. Graph showing the light (blue) and dark (red) samples compared to initial values in location #2 after the first Mississippi Sound three-day experiment 45

43. Graph showing the three-day total of irradiance during the first Mississippi Sound test 45

44. Graph showing the light versus the dark values for CO_2 after the first Mississippi Sound three-day experiment at location #1 46

45. Graph showing the light versus the dark values for CO_2 after the first Mississippi Sound three-day experiment at location #2 46

46. Graph showing the light versus the dark values for CO_2 after the first Mississippi Sound three-day experiment at location #3 47

47. Graph showing the first order kinetics from the first Mississippi Sound test including location #1 (blue), location #2 (green), and location #3 (blue) 47

48. Graph showing the light (blue) and dark (red) samples compared to initial values in location #1 after the second Mississippi Sound three-day experiment 49

49. Graph showing the light (blue) and dark (red) samples compared to initial values in location #2 after the second Mississippi Sound three-day experiment 50

50. Graph showing the light (blue) and dark (red) samples compared to initial values in location #3 after the second Mississippi Sound three-day experiment 50

51. Graph showing the three-day total of irradiance during the second Mississippi Sound test 51

52. Graph showing the light versus the dark values for CO_2 after the second Mississippi Sound three-day experiment at location #1 51

53. Graph showing the light versus the dark values for CO_2 after the second Mississippi Sound three-day experiment at location #2 52

54. Graph showing the light versus the dark values for CO_2 after the second Mississippi Sound three-day experiment at location #3 52

55. Graph showing the first order kinetics from the second Mississippi Sound test including location #1 (blue), location #2 (green), and location #3 (blue) 53

CHAPTER I

RATIONALE

Globally, biomass burning is estimated to produce between 40 and 250 million tons of pyrogenic carbon every year (Jaffe et al., 2013). Historical fire data indicate that since 2002, 25% of recorded vegetation fires within the continental U.S. occurred in the northern Gulf Coast of Mexico (GOM) region (Figure 1). The average size of these fires was 103 acres and contributes an estimated 1 to 2 million tons of pyrogenic C yr^{-1} to the soil carbon pool. Pyrogenic carbon can be divided into: 1) insoluble or particulate fraction (herein referred to as *pPy*C), and 2) a soluble/dissolved fraction (herein referred to as *Py*DOC). Jaffe (2013) estimates that 10.6 to 66 percent of annually produced pyrogenic carbon enters the ocean as dissolved pyrogenic carbon. From this it can be inferred that approximately 0.106 and 1.32 million tons of dissolved pyrogenic carbon enter the GOM each year. Masiello (2004) noted that a comprehensive understanding of the processes accounting for the loss of *py*DOC in general is still needed. While the role of microorganisms on the fate and transformation of both *pPy*C and *Py*DOC has been widely studied, there are significant knowledge gaps concerning the role of abiotic processes and their fate. Current research indicates that despite a general lower susceptibility to biodegradation than their unpyrolyzed equivalents, neither *pPy*C nor *py*DOC is environmentally inert (Shrestha et al., 2010; Cusack et al., 2012; Graneli et al., 1996; Hedges et al., 1997; Kuhlbusch, 1998; Mannino & Harvey, 2004; Middleburg, 1998). For example, *Py*DOC is known to be susceptible to photodegradation (Masiello, 2013). However, very little is known about photodegradation or the fate of *Py*DOC subject to photodegradation. This *py*DOC can complex with contaminants and nutrients

and subsequently, photodegradation could release the complexed nutrients or contaminants (Jonasson, 1999). This degradation of the *Py*DOC has the potential to play a major role in the hypoxic events as well as being a major unknown contributor to CO_2 emission along the northern GOM. A key question is what happens to this pyrogenic carbon once it gets to an aquatic sink like a lake or the ocean? Understanding the fate and transport of this *py*DOC is therefore crucial to deciphering the critical links between fire, biogeochemical cycles and environmental sustainability in the sensitive terrestrial and aquatic ecosystems like the northern GOM.

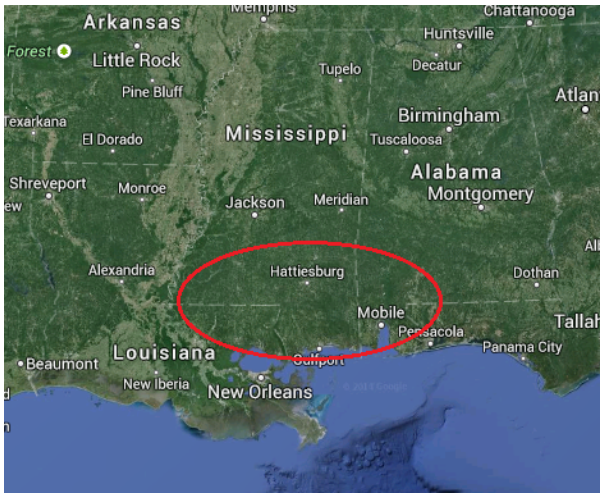

Figure 1. The study site within the northern Gulf of Mexico region (Google Earth Imagery, 2014).

Prescribed burning events, which typically take place during the late winter, followed by increased rain events in the spring, produce optimal conditions for transporting and dissolving *pP*yC. Increases in the average radiation from winter (3 kW h/m^2/day in January) to summer (5 kW h/m^2/day in July) also serve to increase the potential for photodegradation of pyDOC (Figure 2 and 3). Results from preliminary

experiments, 1) indicate that photodegradation of *Py*DOC occurs at a much faster rate than that reported in literature for its biodegradation and 2) pointed to the release of CO_2 as a potential byproduct from the photodegradation of *Py*DOC in aquatic systems. In addition to improving current understanding of carbon cycling, this could have significant implications for deciphering crucial links between fire and nutrient loading as well as feedback mechanisms between climate change and greenhouse gas emissions in subtropical and tropical regions.

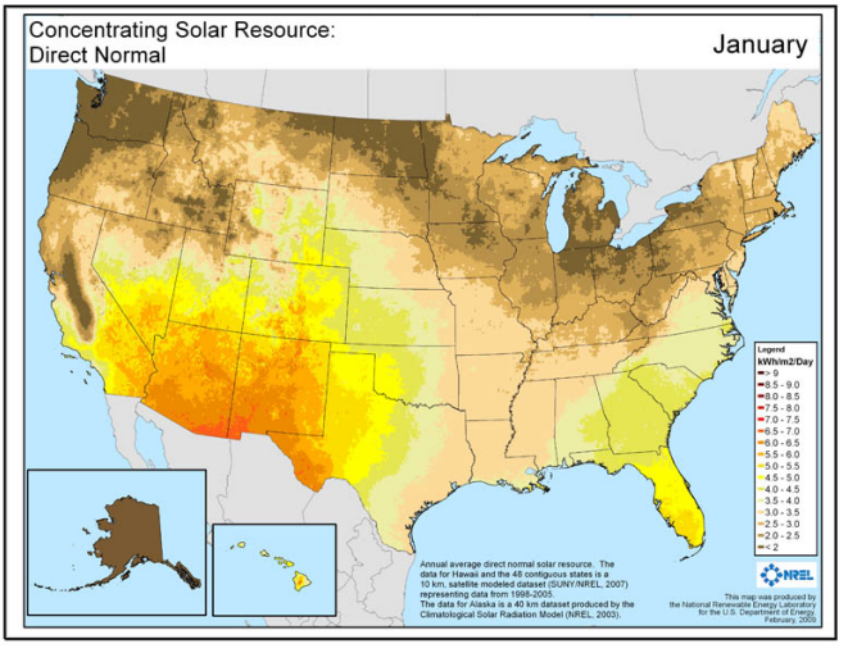

Figure 2. Map showing the average kW h/m^2/day in January for the U.S. (United States Nation Renewable Energy Laboratory, United States Department of Energy, 2003).

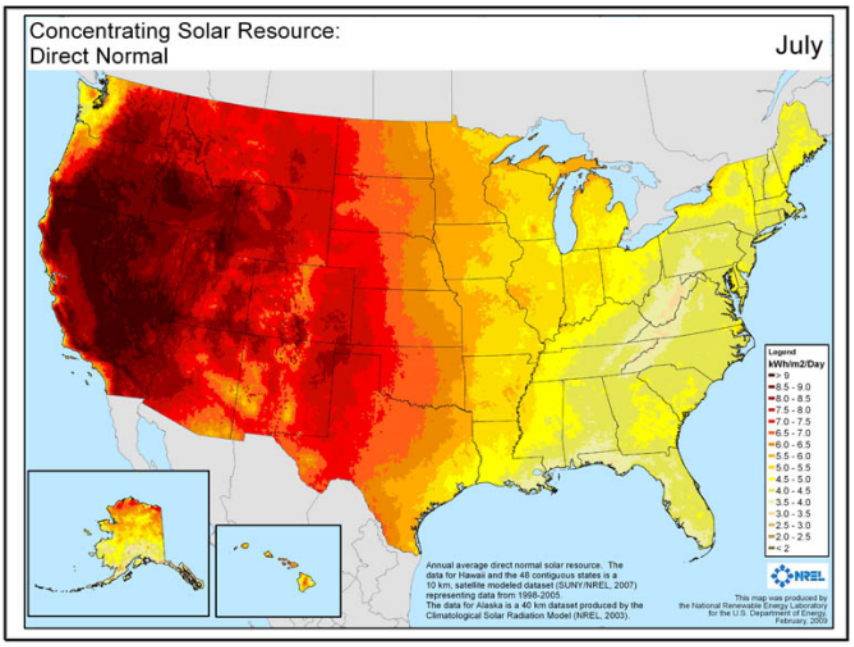

Figure 3. Map showing the average kW h/m^2/day in July for the U.S. (United States Nation Renewable Energy Laboratory, United States Department of Energy, 2003).

CHAPTER II

LITERATURE REVIEW

Efforts to estimate the contribution of pyrogenic carbon to global carbon flux have been a primary focus of *py*C research for the last decade. With new advances in technology and knowledge, new ways to accomplish the task have become available. For the first time, Jaffe et al. (2013) provided an estimate of the global flux of dissolved pyrogenic carbon from terrestrial sources to the ocean through rivers. Jaffe et al. (2013) estimated pyrogenic carbon generated via global biomass burning to be 40 to 250 mega-metric tons (MMT) per year with pyrogenic carbon making up 5-40% of total soil organic carbon. This compares to total global pyrogenic carbon stock in sediments, soils, and waters of 300 to 500 giga-metric tons of carbon. Greater than 2% of marine dissolved organic carbon (DOC) pool has been shown to contain a heat induced molecular signature indicative of terrestrially produced pyrogenic carbon being transported to the oceans (Jaffe et al., 2013). This fact makes the importance of the translocation of pyrogenic carbon from terrestrial systems to the ocean critical. Unfortunately few data on *Py*DOC loads are available for rivers and the quantitative information is too limited to estimate land to ocean fluxes. For their study, Jaffe et al. (2013) looked at 174 freshwater samples throughout the world. They found that the *Py*DOC concentrations varied from 1.94×10^{-3} to 2.77 mg C l^{-1}. The *Py*DOC comprised 0.1 to 17.5% of the DOC. They also found that despite the variability in *Py*DOC and DOC, the concentrations were highly linearly correlated, which is consistent with previous studies. They used this correlation to then convert published data for global river DOC loads into *Py*DOC loads. With this,

they found that about 26.5 MMT of carbon is the annual *Py*DOC flux from land to ocean based on a riverine DOC of 250 MMT of carbon per year.

Some areas of *PyC* exploration, such as trace element speciation by photooxidation, have yet to be fully understood. Shiller et al. (2006) studied the effects of photodegradation of fluvial DOC on dissolved trace elements using water collected from the Pearl River near Stennis Space Center on the coast of Mississippi. Shiller et al., (2006) chose a sterile filtration approach through 0.22 micrometer to minimize biological effects. They separated 20L of sampled water into 5L Teflon bags, half of which were covered in tinfoil as dark controls. These bags were chosen because of they transmitted over 80% of the incident UV light. Shiller et al. (2006) used temperature controlled Plexiglas incubators kept outdoors in ambient sunlight. Every 5 days during the incubation, two dark and two light bags were taken around noon for sampling. Results from the data show that some elements, such as Fe, did show significant changes due to the light exposure. Dissolved Fe decreased continuously and the organically complexed Fe was released during photodegradation. The released Fe was then precipitated as additional colloidal FeOOH. Ce, Cu, Cr, Pb, V, and U also showed a decrease in their retention by an anion exchange column.

Mitra et al. (2002) examined the quantities, sources, and implication of *py*DOC from the Mississippi River. The paper states that in 1999 the Mississippi River discharged 5% of the pyDOC buried annually in the oceans. Results such as these demonstrate the importance of understanding the fate of this excess carbon and its implication for the northern Gulf of Mexico regions.

Because most aquatic ecosystems exhibit some seasonal variation, it is likely that DOC concentrations and photooxidation rates also vary seasonally. Suhett et al. (2007) studied the impact of seasonal rainfall events with the seasonal changes of DOC photooxidation rates in a tropical humic coastal lagoon (Comprida Lagoon, north of Rio de Janeiro State, Brazil). Comprida Lagoon can reach DOC concentrations close to 5 mmolC L^{-1} with more than 90% of total carbon being humic carbon. Suhett et al. (2007) note that since DOC is involved in linking the hydrosphere and biosphere, it has the potential to affect global climate changes. Samples were collected over seven days between March 2003 and November 2004. Samples were placed in UV transparent culture bags, noting that the photooxidation rates would be underestimated because the bags transmit only 35% of the UV light. Rainfall data was collected from a meteorological station at a local farm. The rainfall followed the general seasonal pattern for the area with the rainy season from October to March. In general, during the rainy season, Suhett et al. (2007) concluded that DOC values were high, and in the drier months the DOC was lower. These implications are similar to predictions for this study as it is predicted that *py*DOC concentrations increase in the spring and with rainfall and therefore photodegradation and the loss of *py*DOC will increase in the spring and early summer. Also this study will likely produce underestimated data due the glass crimp vials.

Cory et al. (2007) highlights an important extensive source of dissolved organic matter that originates in the Arctic tundra. They studied the importance of this organic matter because of its ease of translocation to the Arctic Ocean. Cory et al. (2007) emphasizes that photodegradation processes predominantly control the chemical

character of Arctic surface waters and that more studies must be conducted before considering the ultimate fate of dissolved organic matter.

Cory et al. (2013) note that the high-latitude soils previously discussed in Cory et al. (2007) currently store at least twice the carbon found in the atmosphere. The paper notes that recent increases in soil temperatures have allowed for thawing of soils and microbial respiration of previously frozen carbon. Along with this microbial respiration, photodegradation of carbon as the soil thaws could produce sizable quantities of CO_2 as well. Cory et al. (2013) states that once thawed and exposed, the fate of *py*DOC is unknown and will depend on its reactivity to the combined effects of sunlight and microbial processing.

Moran et al. (2000) noticed that photodegradation processes that induce changes in natural dissolved organic matter can influence many aspects of carbon cycling in marine environments. Specifically, as photodegradation is occurring, a loss of color known as photobleaching occurs that affects the optical properties of seawater and influences penetration of ultraviolet and photosynthetically active wavelengths. This loss of color could affect the depth at which *py*DOC can be degraded which is discussed here in Chapter VII. More penetration of ultraviolet radiation would result in underestimated degradation rates.

Corey et al. (2014) noted that CO_2 emissions from inland surface waters to the atmosphere are as large as the net carbon transfer from the atmosphere to earth's surface. Cory et al. (2014) studied how sunlight controlled the processing of carbon in arctic freshwaters and found that CO_2 released via photodegradation accounts for around one-third of the total CO_2 released from surface waters in the arctic. The article also notes that

photodegradation, as opposed to bacterial respiration, accounts for between 70-95% of total DOC processed in arctic lakes and rivers.

CHAPTER III

METHODS

The *py*DOC for both laboratory and field-scale experiments was extracted from natural charcoal collected from a pine (*Pinus echinata*) plantation in south-central Mississippi. Charcoal from pine was selected because pine trees dominate much of the landscape in the northern GOM region and are subject to frequent prescribed burning cycles as a management strategy. For example, the pine plantation from which the charcoal was collected is burned on a yearly cycle. To extract the *py*DOC the charcoal was dried to constant weight at 75^{o}C, grounded and sieved to pass through a 150 μm sieve. 100mg sieved charcoal was then combined with 10ml of 1M KOH, and the resulting suspension filtered through a 20*nm* filter. The filtrate is operationally defined as containing the dissolvable humic and fulvic fractions of the *Py*C or the *py*DOC fraction. The *py*DOC solution was diluted with UV-treated 18.0MΩ water (TOC content < 30 ppb) to produce a stock solution of ~7.25 mg DOC L^{-1} for use in all further experiments. Stock solution was made fresh each day an experiment is conducted. Samples were analyzed using UV visible spectrophotometry for absorbance, and gas chromatography for CO_2 analysis. A wavelength of 365nm was selected for the UV visible spectrophotometer because of the four tested wavelengths (λ_{abs} = 254, 302, 365, 550) it was shown to be best correlated to measured *py*DOC (r^2 = 0.999).

Preliminary exploratory laboratory experiments testing photodegradation involved two flasks of stock solution, one being exposed to the sun and the other wrapped in aluminum foil as a control. Samples were taken at regular intervals and tested for absorbance. Using a total organic carbon (TOC) analyzer from the University of Southern

Mississippi Gulf Coast Research Center, a standard curve between DOC concentration and absorbance. DOC concentrations could then be calculated from the absorbance values by using the formula, y = 110.27x (y = DOC concentration and x = absorbance). The DOC levels were then compared to irradiance levels from the Southern Miss Lake Thoreau weather station. From these comparisons, a graph showing the levels of irradiance and the corresponding loss of DOC was created to be able to predict the loss of DOC with a known irradiance. Further methods for specific tasks will be explained in each chapter.

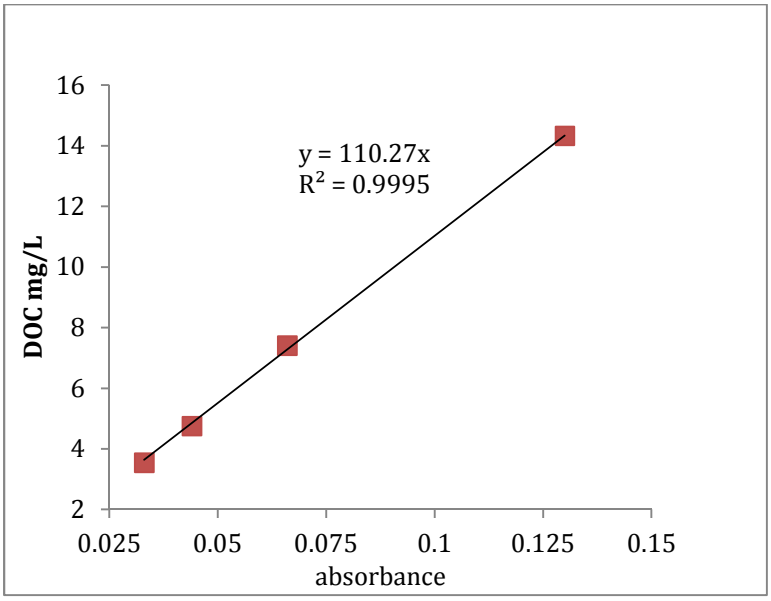

Figure 4. Graph showing the relationship of absorbance values to DOC concentrations.

CHAPTER IV

INFLUENCE OF RADIATION INTENSITY ON PHOTODEGRADATION OF *py*DOC AND CO_2 PRODUCTION

Introduction

To analyze photodegradation of *py*DOC, a set of controlled field experiments were conducted on the Lake Thoreau Environmental Center extension to the campus of The University of Southern Mississippi. The stock solution was prepared as described in the methods section and 10ml crimp vials were filled with 7.5ml of the stock solution, sealed, and placed in direct sunlight next to the Lake Thoreau weather station. Half of the vials were covered with aluminum foil to be used as a dark controls. Three light and three dark samples were then taken hourly during ten hour exposure periods. Samples were immediately analyzed via gas chromatography for headspace CO_2, and via UV-visible absorption spectrophotometry (λ_{abs} = 365 nm) for *py*DOC. The pyDOC fraction was determined using the standard curve in Figure 4. The primary environmental parameter of interest that was considered was solar irradiance. All of these factors were taking into account when providing conclusions to the study.

Figure 5. Samples being exposed to the sun (right) along with samples wrapped in aluminum foil (left) at the base of the Lake Thoreau weather station (Photography by John Thomas Howell, 2014).

Results and Discussion

Effects of solar radiation intensity on pyDOC concentration

Figures 6,7, and 8 show the relationship between the solar irradiance and loss of *py*DOC. Data for solar irradiance are integrated values corresponding to the total exposure time up to a given *py*DOC sampling interval. For example, sampling for *py*DOC in these experiments occurred every hour for ten hours per day, hence solar irradiance at 10 h indicate total solar irradiance to which the samples were exposed. At each sampling interval, absorbance was measured, values converted to *py*DOC concentration and presented as C/C_o versus time, where C is the *py*DOC concentration at

a given sampling time, t and C_o is the initial *py*DOC at time, 0. Total solar irradiance for Day 1 (Test #1; Figure 6), Day 2 (Test #2; Figure 7) and Day 3 (Test #3; Figure 8) were 5.41, 3.59 and 2.79 kW h/m^2, respectively. These values were consistent with expected ranges for solar irradiation intensity across the northern Gulf of Mexico (NGOM) within a given year (Figure 2 and 3). The decline in C/C_o with time and solar irradiance, for light samples on a given test day were indicative of *py*DOC photodegradation. The lack of change in C/C_o in dark controls indicated no photodegradation and suggested that changes in temperature and microbial degradation of *py*DOC had no significant effect on *py*DOC loss in these experiments.

Both quantity and rate of *py*DOC photodegradation was affected by radiation intensity. Approximately 52, 44 and 40% of pyDOC was photodegraded within a 10 h period when integrated solar irradiance was 5.41, 3.59 and 2.79 kW h/m^2, respectively. First-order kinetic analysis (Figure 11) showed that rate of photodegradation also increased with solar irradiance. For example, the first-order rate constant (k) for the photodegradation of *py*DOC was 0.080 h^{-1} for Test #1 (solar irradiance = 5.41 kW h/m^2) compared to 0.060 h^{-1} for Test #2 (solar irradiance = 3.59 kW h/m^2) and 0.054 h^{-1} for Test #3 (solar irradiance = 2.79 kW h/m^2). This suggested that photodegradation half-life for *py*DOC (calculated as ln(2)/k) was between 9 and 13 hours (0.36-0.54 days). These values are approximately an order of magnitude lower than the 30-40 days reported by Norwood et al. (2013) for half-lives of *py*DOC biodegradation. Differences in photodegradation and biodegradation half-lives were consistent with Amon and Benner (1996) who found that photochemical consumption of DOC in Amazonian rivers occurred at rates around seven times that for microbial consumption. Such large kinetic

differences suggest that photodegradation (rather than microbial degradation) was most likely to regulate *py*DOC bioavailability in fire-impacted aqueous environments.

Influence of solar radiation intensity on CO_2 evolution during pyDOC photodegradation

Production of CO_2 was affected by the level of solar radiation. An increase in CO_2 of more than 11.5 times the dark control was observed in test #1 with overall radiation of 5.4 kW h/m^2/day. Virtually no increase in headspace CO_2 was found relative to the control in test #2 while the overall radiation was only 3.6 kW h/m^2/day. With the major increase in CO_2 coming at around 8 hours of exposure in test #1, a possible threshold of around 4 kW h/m^2/day was suggested for initiation of CO_2 production. Since CO_2 is a greenhouse gas, this large increase could produce the potential of harsh environmental effects. As was discussed previously, the potential implications of this greenhouse gas are extensive. With large amounts of CO_2 entering the atmosphere from a previously little to unknown source, current models attempting to predict climate change could be influenced as well as short-term weather models. With more than eleven times more headspace CO_2 after just 10 hours of exposure to sunlight, implications of increasing wildfires and prescribed burning events become a more pressing issue.

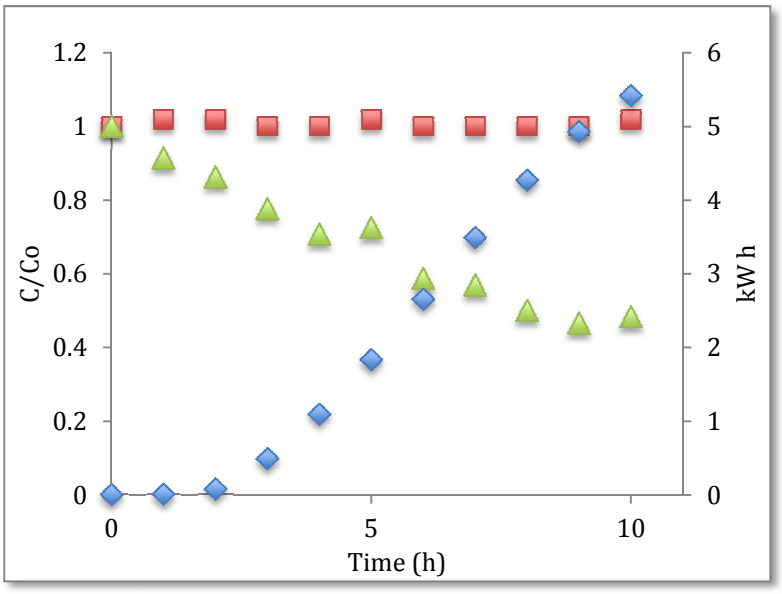

Figure 6. Test #1 run at the Lake Thoreau weather station showing the light (green) and dark (red) samples compared to initial values along with the irradiance levels (blue).

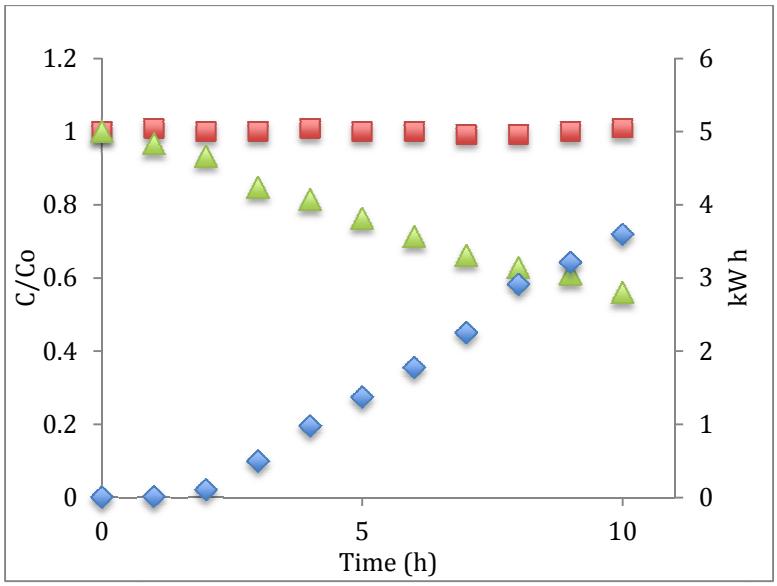

Figure 7. Test #2 run at the Lake Thoreau weather station showing the light (green) and dark (red) samples compared to initial values along with the irradiance levels (blue).

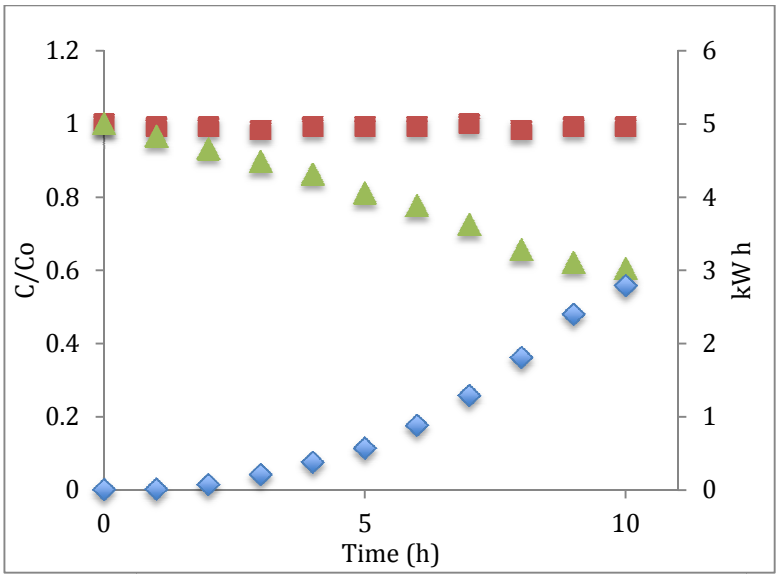

Figure 8. Test #3 run at the Lake Thoreau weather station showing the light (green) and dark (red) samples compared to initial values along with the irradiance levels (blue).

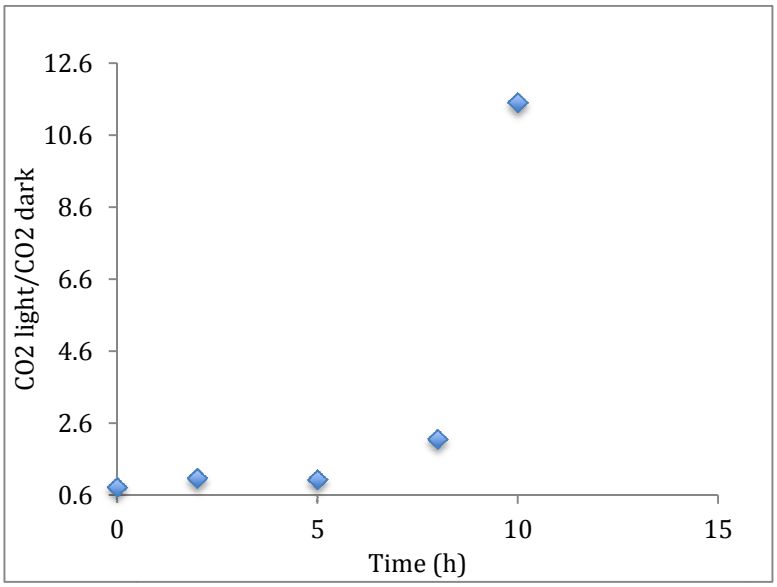

Figure 9. Graph showing the light versus the dark values for CO_2 from test #1.

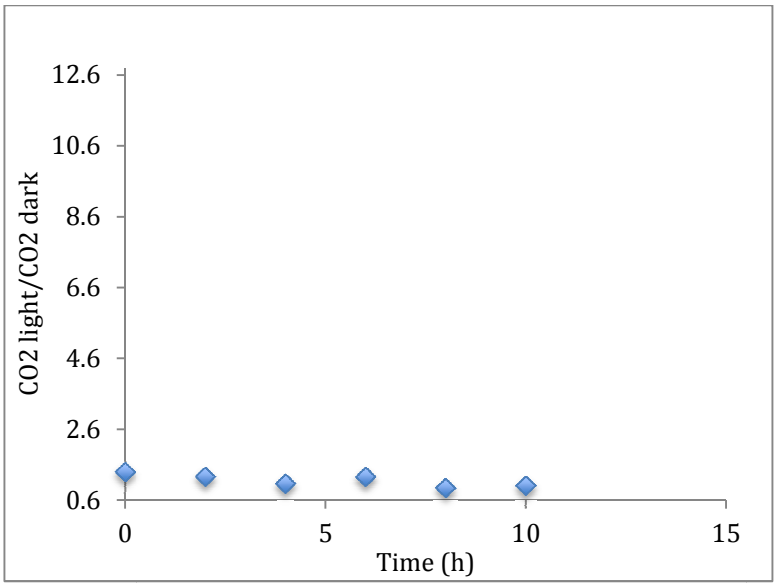

Figure 10. Graph showing the light versus the dark values for CO_2 from test #2.

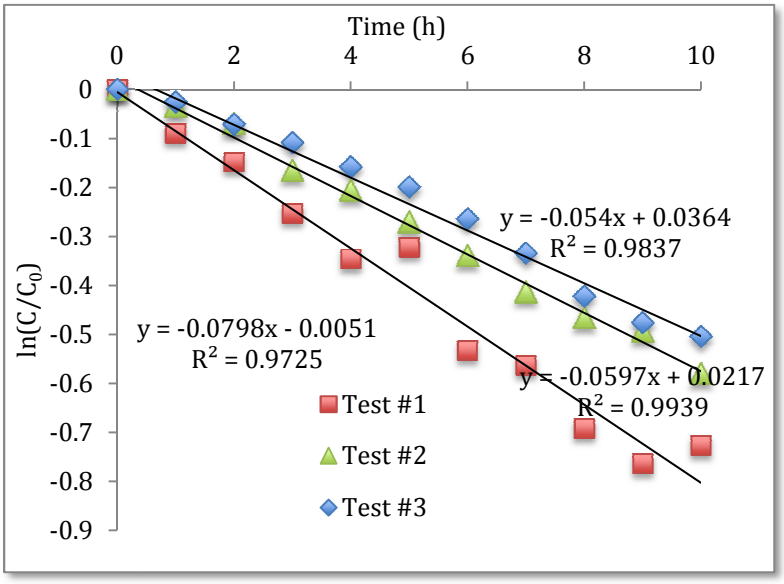

Figure 11. Graph showing the first order kinetics from tests #1 (red), #2 (green), and #3 (blue).

CHAPTER V

ASSESSING THE INFLUENCE OF SALINITY AND DEPTH BELOW THE SURFACE ON PHOTODEGRADATION

Introduction

Many factors have the potential to influence photodegradation rates and byproducts. Two factors that were explored in this study were photodegradation rates at varying depths below the surface of the water, and photodegradation rates and byproduct with the incorporation of salinity. To test the influence of depth on the rate of photodegradation, the stock solution described in Chapter II was sealed in crimp vials. The sample holding apparati described in Chapter V were utilized by placing all three in the same location at depths of 3, 6, and 12 inches below the surface of Lake Thoreau. Samples were then collected every two and a half hours from 7:00am to 7:30pm. The samples were returned to the lab and analyzed using UV visible spectrophotometry.

When testing photodegradation in the Gulf of Mexico, it seems necessary to assess the influence of salt on photodegradation. Therefore, and experiment was designed to compare photodegradation of the stock solution to a solution diluted with water from the Gulf of Mexico. The experiment began by preparing the typical stock solution described in Chapter II. Then a similar solution was made, but instead of diluting with DI water, it was diluted with water collected from the Gulf of Mexico. Another solution was made by diluting with equal amounts of DI water and water from the Gulf of Mexico. This essentially allowed the testing of a freshwater solution, a brackish water solution, and a saltwater solution. The experiment was conducted next to the weather station at the Lake Thoreau research center of Southern Miss. The three different solutions along with

corresponding control samples were exposed to sunlight for a full day, sampling every two and a half hours from 7:00am to 7:30pm. In the lab, the samples were analyzed with a gas chromatograph and a UV visible spectrophotometer.

Depth Test Results

The experiment to determine the influence of depth took place on a very sunny day with a total irradiance of 6.2 kW h/m^2 during the exposure. At three inches, a total of 14.1% of the *py*DOC was lost due to photodegradation with no substantial loss in the control sample. At a depth of six inches the samples lost a total of 10.3% of the *py*DOC and at twelve inches the samples lost only 5.9% the their *py*DOC. Because sunlight disperses at the waters surface, the deeper in the water column, the less light. From this data, a graph was created comparing the percent loss of *py*DOC to the depth below the water surface. This graph allows the prediction of the loss of *py*DOC at any given depth. From the graph (Figure 15), it is observed that below two feet, virtually no *py*DOC is expected to degrade due to photodegradation, with the graph showing less than a 2% loss at twenty-four inches. It can be assumed that below two feet in Lake Thoreau, any degradation of *py*DOC over 2% can be attributed to microbial degradation.

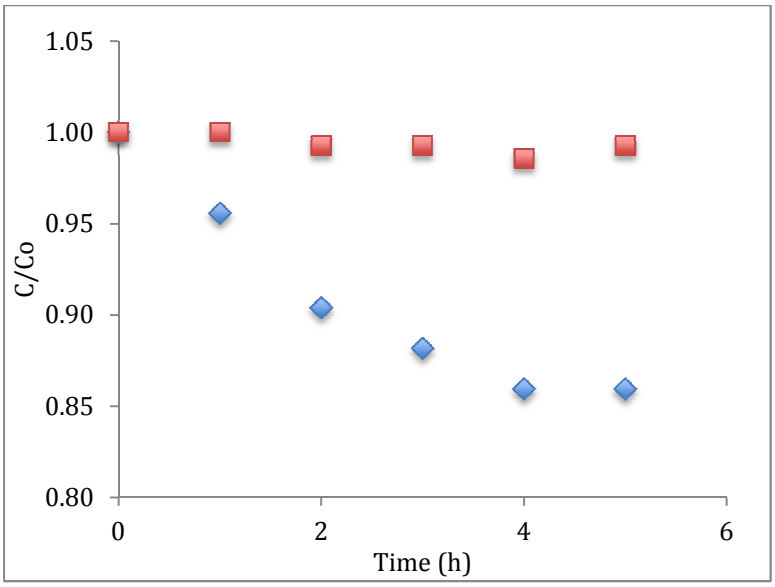

Figure 12. Graph showing light (blue) and dark (red) samples compared to initial values at 3 inches below the surface of Lake Thoreau.

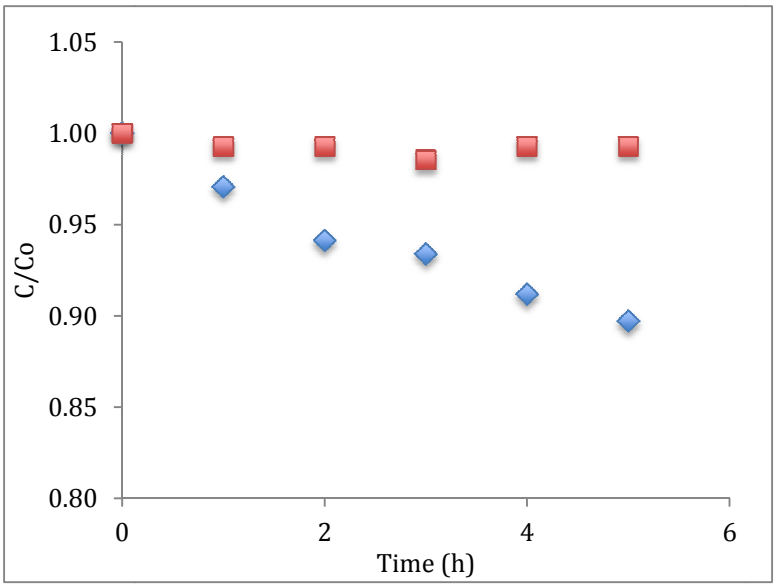

Figure 13. Graph showing light (blue) and dark (red) samples compared to initial values at 6 inches below the surface of Lake Thoreau.

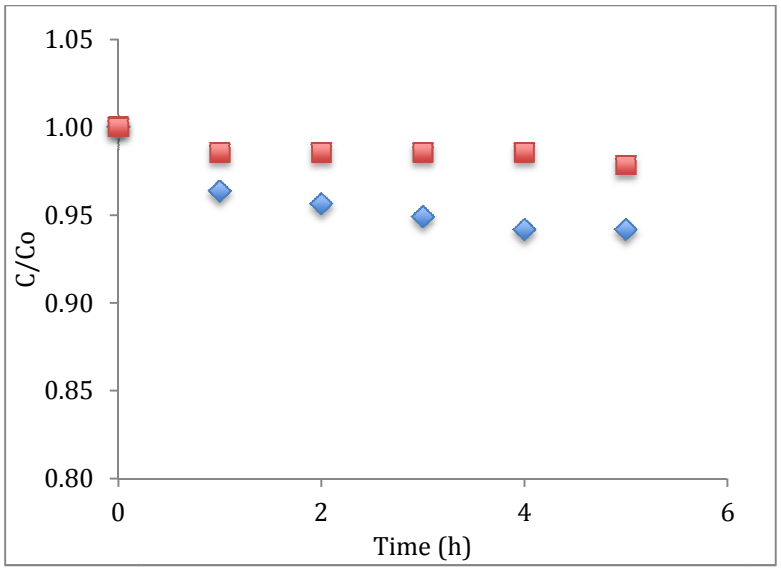

Figure 14. Graph showing light (blue) and dark (red) samples compared to initial values at 12 inches below the surface of Lake Thoreau.

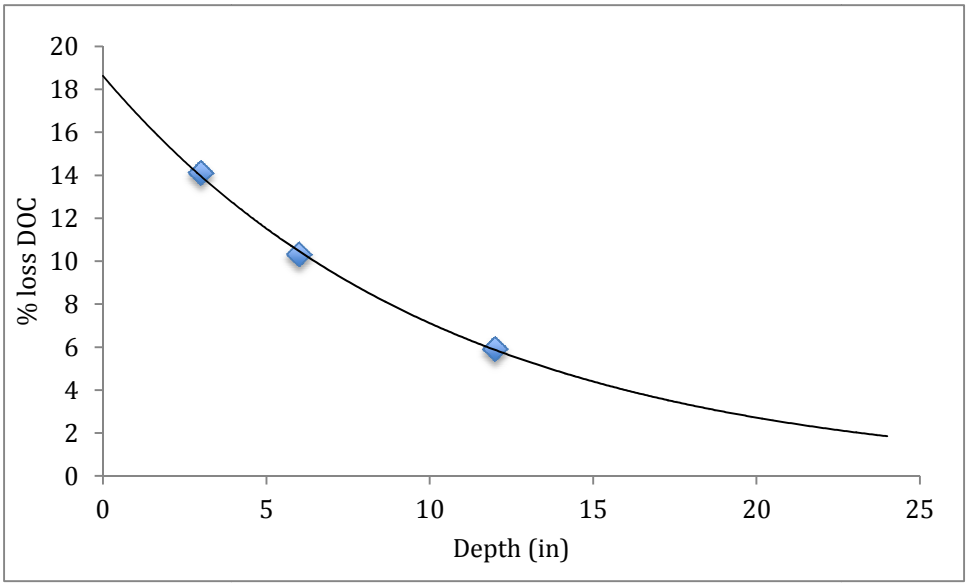

Figure 15. Graph showing the percent loss of PyDOC with depth.

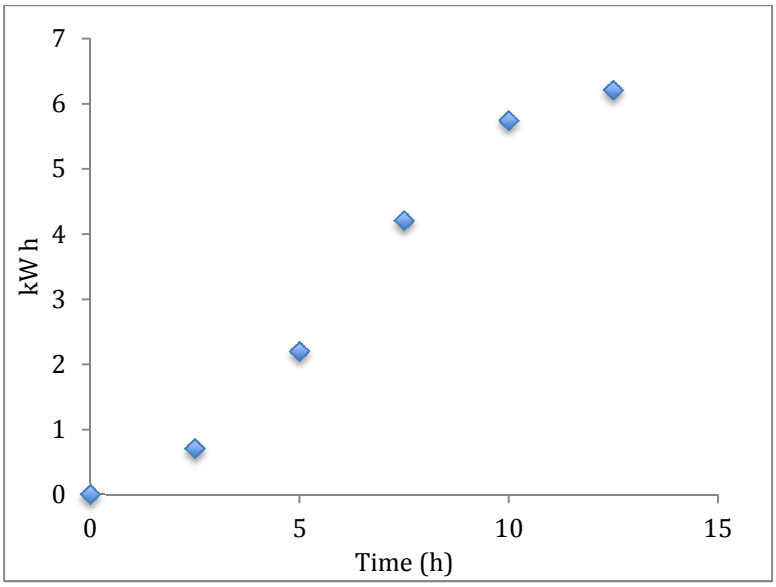

Figure 16. Graph showing the integrated irradiance during the depth tests.

Salinity Test Results

With 5.3 kW h/m^2 of irradiance on the day of test, all of the tests analyzing salinity showed around a 60% loss of *py*DOC. Using the gas chromatograph it was found that no CO_2 was produced in any of the samples for this experiment. This was consistent with previous results, because the total irradiance for the day just over the estimated threshold for CO_2 production of 5 kW h/m^2. The samples with no salt (diluted in DI water) and ½ salt (diluted with equal parts DI water and half Gulf of Mexico saltwater) showed exactly a 60% loss in *py*DOC while the sample with salt (diluted with Gulf of Mexico saltwater) lost 61.3% of its *py*DOC. While these are large losses in *py*DOC, no variability was observed in the rates or products or the degradation, suggesting that salinity does not have an effect on photodegradation rates or the degraded byproducts.

First-order kinetic analysis (Figure 21) showed that rate of photodegradation increased with solar irradiance. For example, the first-order rate constant (k) for the photodegradation of *py*DOC was 0.0765 h^{-1} for No Salt (solar irradiance = 5.41 kW h/m^2)

compared to 0.060 h^{-1} for Test #2 (solar irradiance = 3.59 kW h/m^2) and 0.054 h^{-1} for Test #3 (solar irradiance = 2.79 kW h/m^2). This suggested that photodegradation half-life for *py*DOC (calculated as ln(2)/*k*) was between 9 and 13 hrs (0.36-0.54 days). These values are approximately an order of magnitude lower than the 30-40 days reported by Norwood et al. (2013) for half-lives of *py*DOC biodegradation. Differences in photodegradation and biodegradation half-lives were consistent with Amon and Benner (1996) who found that photochemical consumption of DOC in Amazonian rivers occurred at rates around seven times that for microbial consumption. Such large kinetic differences suggest that photodegradation (rather than microbial degradation) was most likely to regulate *py*DOC bioavailability in fire-impacted aqueous environments.

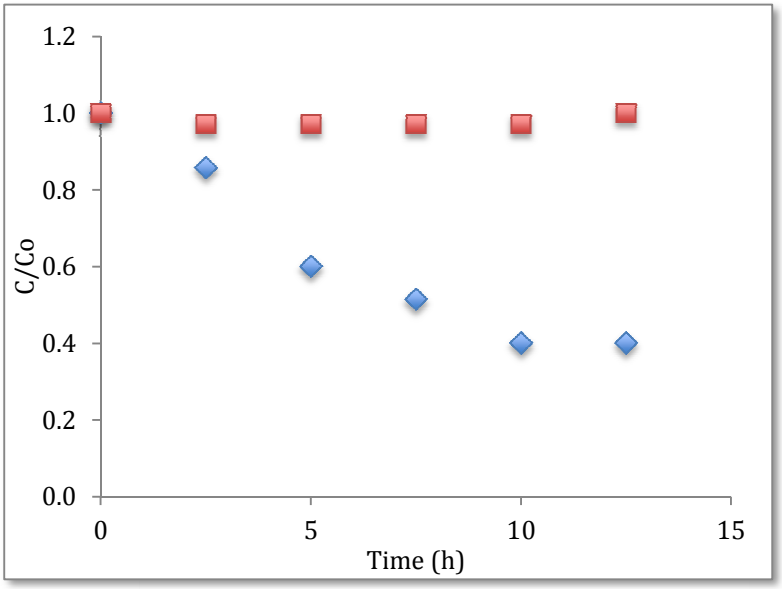

Figure 17. Graph showing light (blue) and dark (red) samples compared to initial values in a solution of DI water.

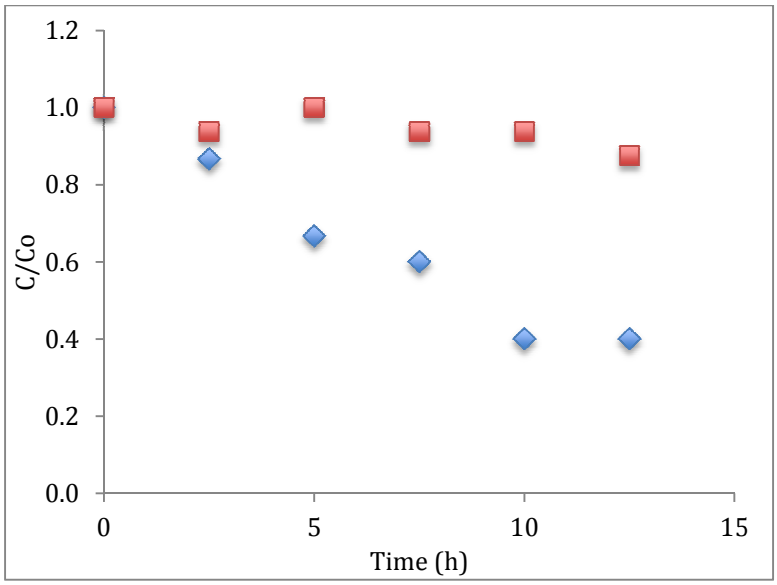

Figure 18. Graph showing light (blue) and dark (red) samples compared to initial values in a solution of salt and DI water.

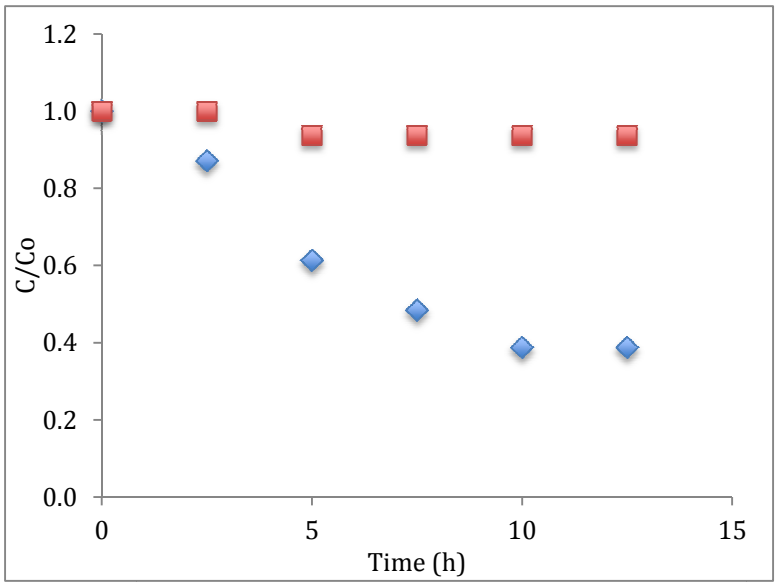

Figure 19. Graph showing light (blue) and dark (red) samples compared to initial values in a solution of saltwater.

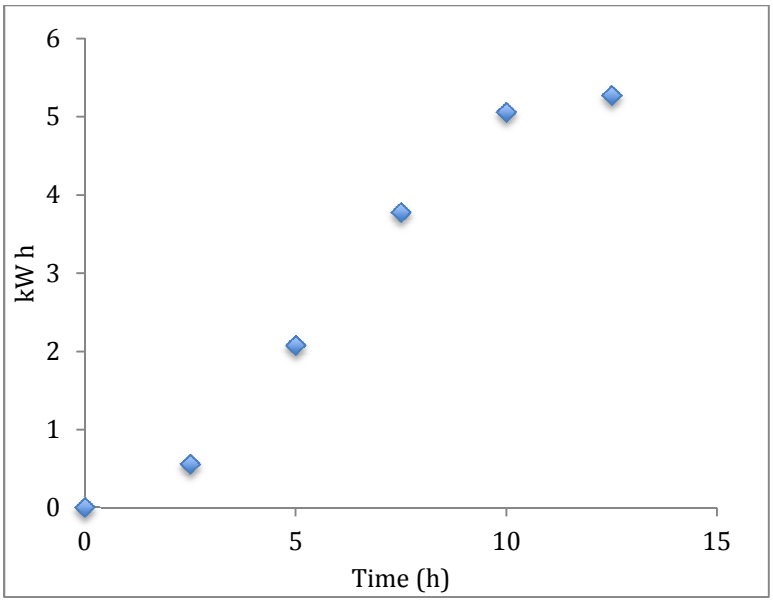

Figure 20. Graph showing the irradiance during the salinity tests.

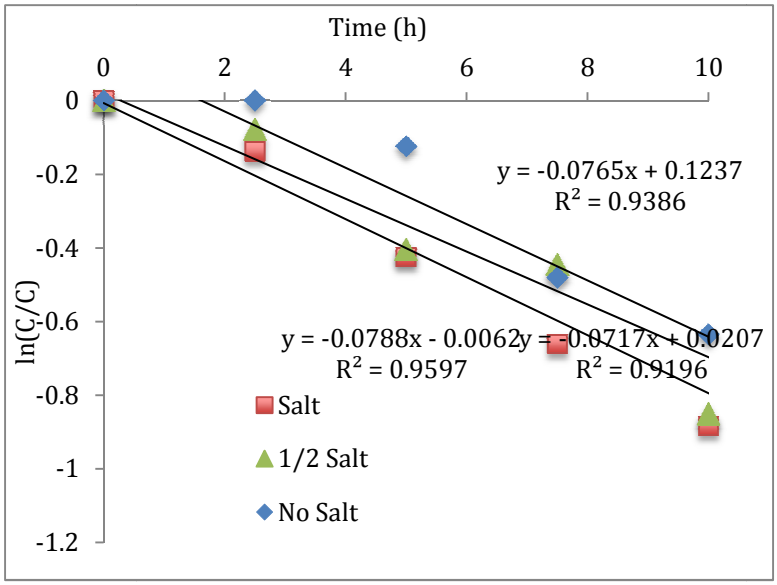

Figure 21. Graph showing the first order kinetics from the salinity including the no salt test (blue), ½ salt test (green), and the salt test (blue).

CHAPTER VI

ASSESSMENT OF *py*DOC PHOTODEGRADATION AND CO_2 IN A FRESHWATER SYSTEM

Introduction

With most of the prescribed burning taking place in the late winter and early spring, the ground is left bare for the spring. The lack of ground cover to secure the fresh char provides allows spring rains that frequent the northern GOM region to wash the char into the freshwater lakes and rivers. With freshwater lakes and rivers being the first bodies of water to be introduced to the annual flux of *Py*C, it is important to study photodegradation in different aspects of the freshwater system. This set of experiments focuses on photodegradation at varying distance from the shoreline of a typical freshwater lake in southern Mississippi as well as exploring photodegradation over longer time spans.

These experiments began with designing and building a sample holding apparatus to hold samples in vials below the water surface of a lake. The design was a plywood board with rubber bands stapled to the top to hold the vials with the stock solution described within Chapter III. The board was then attached to a brick, which was lowered to the bottom of the lake, suspending the board so that the vials hovered an inch below the surface of the water. Samples containing the stock solution were attached to the sampling apparatus and placed approximately 5 (location #1), 25 (location #2), and 50 yards (location #3) from the shoreline of Lake Thoreau. Fifty yards corresponded to roughly the middle of the lake. Vials were taken from each board over three days at 7am, 11am, 3pm, and 7pm on each sampling day. This four-hour time interval provided the

right amount of detail to thoroughly explore photodegradation in the freshwater lake. After each sample was taken, the headspace CO_2 was measured by gas chromatography. Then the vials were decrimped and the solution phase analyzed by UV-vis spectrophotometry in absorbance mode (λ_{abs} = 365 nm). The vials were then tested for pH and EC and results compared to the irradiance levels measured during the three-day period. This three-day experiment was then repeated for a total of two experiments.

Figure 22. Picture of the sample holding apparatus in Lake Thoreau (Photography by John Thomas Howell, 2014).

Figure 23. Samples attached to sample apparati with rubberbands (Photography by John Thomas Howell, 2014).

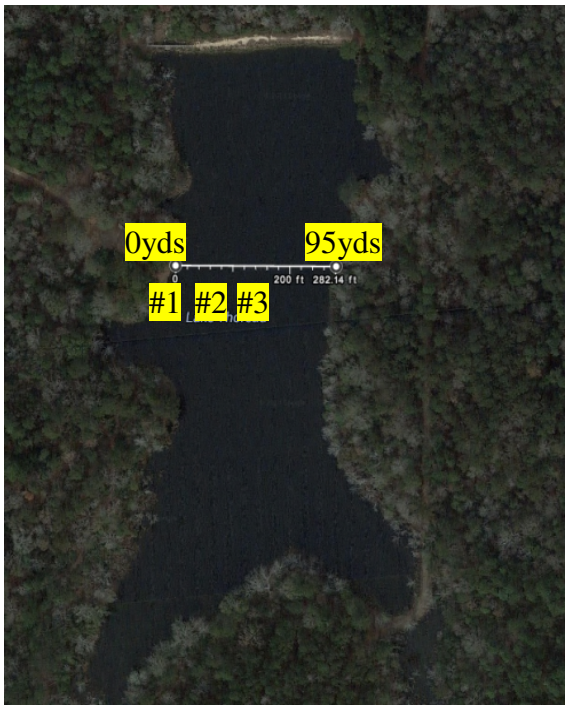

Figure 24. Arial image showing the design of the three locations used in Lake Thoreau (Google Earth Imagery, 2014).

Experiment #1 Results and Discussion

Data for solar irradiance are integrated values corresponding to the total exposure time up to a given *py*DOC sampling interval. For example, sampling for *py*DOC in these experiments occurred every four hours for sixty hours (three days) hence solar irradiance at 60 h indicate total solar irradiance to which the samples were exposed. At each sampling interval, absorbance was measured, values converted to *py*DOC concentration and presented as C/C_o versus time, where C is the *py*DOC concentration at a given sampling time, t and C_o is the initial *py*DOC at time, 0. Total solar irradiance for Day 1, Day 2, and Day 3 were 4.33, 6.06, and 6.06 kW h/m^2, respectively. These values were consistent with expected ranges for solar irradiation intensity across the NGOM within a given year (Figures 2 and 3) as well as comparable to the tests done at the weather station. The decline in C/C_o with time and solar irradiance, for light samples on a given test day were indicative of *py*DOC photodegradation. The increase in absorbance in the dark controls, although small, suggested minor microbial growth over the three day experiments.

Both quantity and rate of *py*DOC photodegradation were affected by radiation intensity. Approximately 15% (location #1; Figure 14), 12% (location #2; Figure 15), and 18% (location #3, Figure 16) of *py*DOC was photodegraded over a 60 h period when total solar irradiance was 16.45 kW h/m^2, respectively. These results were not consistent with previous experiments as the experiments at the weather station produced *py*DOC losses of 52%, 44%, and 40% over just 10h with irradiance levels of 5.4, 3.5, and 2.7 kW h per day. This inconsistency was expected as the samples were being exposed below the water surface of Lake Thoreau. After 12h, the samples in Lake Thoreau saw an average loss of 10% with an irradiance of 4.3 kW h/m^2, which is comparable to the experiments at the

weather station. Therefore, according to these results photodegradation accounts for almost 80% less degradation just an inch below the surface of Lake Thoreau. Slight variations in degradation between the locations were noticed with less degradation in location #2 (approximately 25 yards from shore) and the most degradation in location #3 (approximately 50 yards from shore). These variations can be explained because location 3 receives sun in the afternoon longer when irradiance levels are highest, while location 1 receives the most morning sun when irradiance levels are lower. Loss of *py*DOC was relatively continuous on days one and two, but slowed severely on day three with results showing virtually zero loss of *py*DOC in all locations. These results represent a potential threshold that slows the photodegradation after a certain percentage of the *py*DOC is lost.

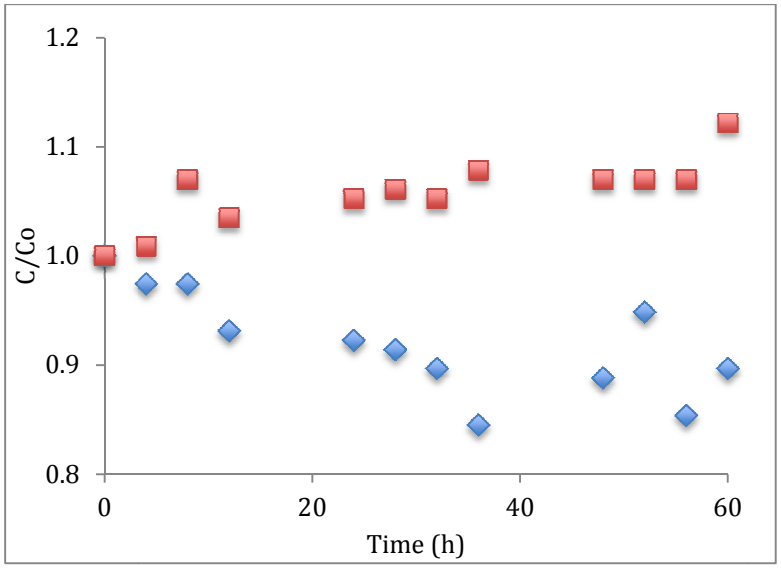

Figure 25. Graph showing the light (blue) and dark (red) samples compared to initial values in location #1 after the first Lake Thoreau three-day experiment.

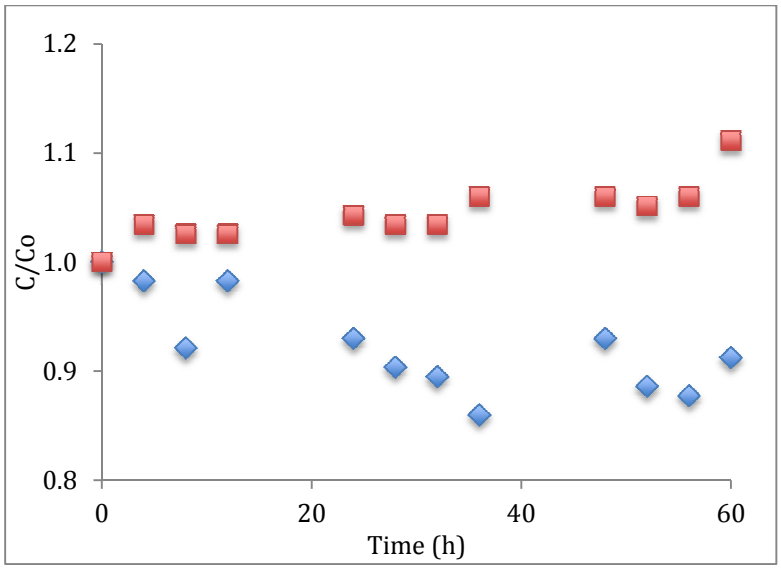

Figure 26. Graph showing the light (blue) and dark (red) samples compared to initial values in location #2 after the first Lake Thoreau three-day experiment.

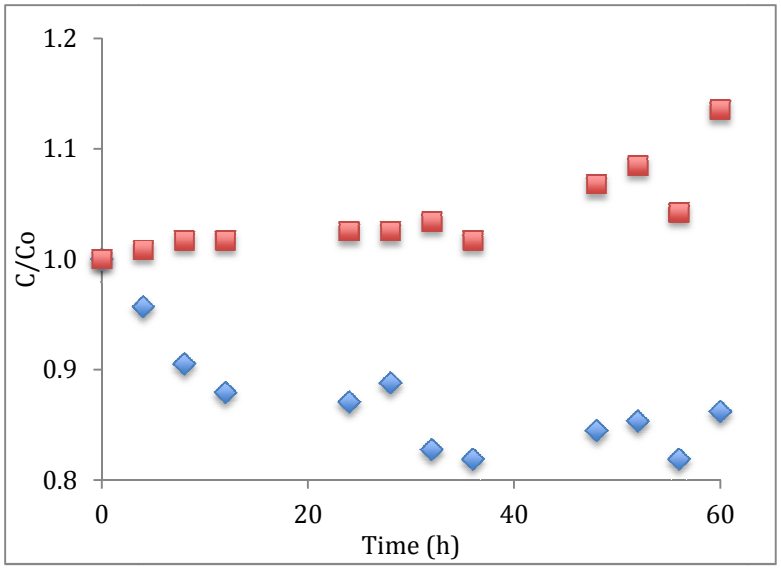

Figure 27. Graph showing the light (blue) and dark (red) samples compared to initial values in location #2 after the first Lake Thoreau three-day experiment.

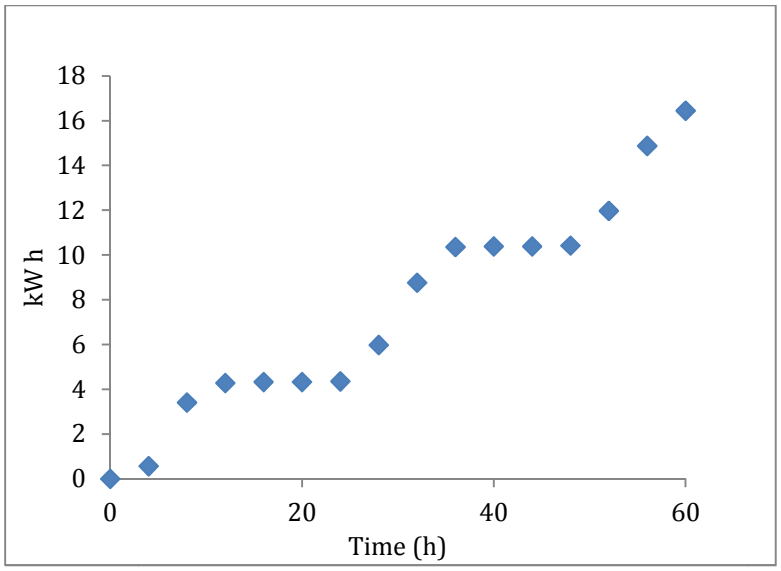

Figure 28. Graph showing the three-day total of irradiance during the first Lake Thoreau test.

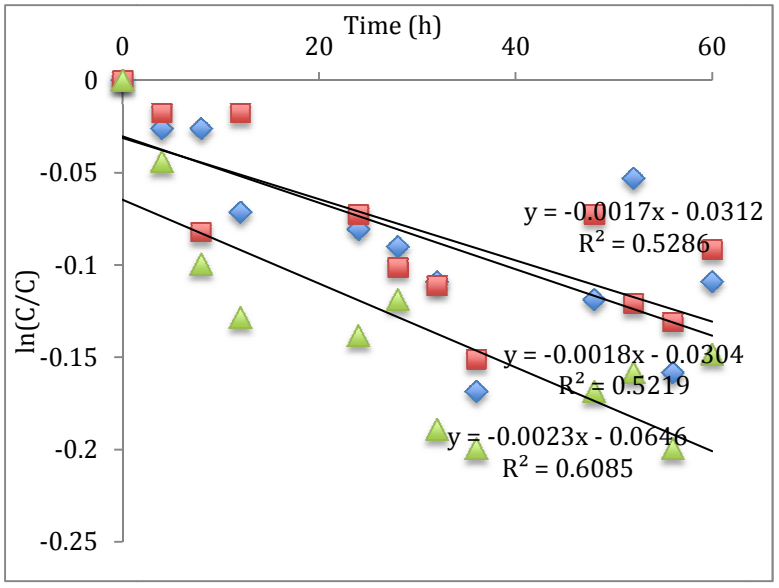

Figure 29. Graph showing the first order kinetics from the first Lake Thoreau test including location #1 (blue), location #2 (green), and location #3 (blue).

Experiment #2 Results and Discussion

As in EXPERIMENT #1 sampling for *py*DOC in these experiments occurred every four hours for sixty hours (three days) hence solar irradiance at 60 h indicate total

solar irradiance to which the samples were exposed. At each sampling interval, absorbance was measured, values converted to *py*DOC concentration and presented as C/C_o versus time, where C is the *py*DOC concentration at a given sampling time, t and C_o is the initial *py*DOC at time, 0. Total solar irradiance for Day 1, Day 2, and Day 3 were 7.07, 7.35, and 5.75 kW h/m^2, respectively. These values were again consistent with expected ranges for solar irradiation intensity across the NGOM within a given year (Figure 2 and 3). The values being on the higher end of the range on days one and two, was contributed to the extreme sunniness during the first two days. The decline in C/C_o with time and solar irradiance, for light samples on a given test day were indicative of *py*DOC photodegradation. The increase in absorbance in the dark controls, although small, again suggested minor microbial growth over the three day experiments.

Both quantity and rate of *py*DOC photodegradation was affected by radiation intensity. Approximately 30, 35, and 30% of pyDOC was photodegraded at the three different locations over a 60 h period when total solar irradiance was 20.17 kW h/m^2, respectively. These values increased slightly compared to the first Lake Thoreau experiment because of the higher solar irradiance values. Slight variations in degradation between the locations was noticed with more degradation in location #2 (approximately 25 yards from shore) and the equal degradation in locations #1 and #3. Loss of pyDOC was relatively continuous on days one and two, but slowed slightly on day three with results showing virtually zero loss of pyDOC in all locations.

Variations in headspace CO_2 concentrations confirmed that the production of CO_2 was also affected by irradiance. A steady increase in CO_2 production led to around twice as much CO_2 in the samples in all locations after three days of exposure. This is

inconsistent from the gas chemistry results from the weather station experiments that showed a potential threshold around 4 kW h/m^2 for CO_2 production and then a major increase to more than 10 times the initial CO_2 in just ten hours. The inconsistency is likely due to the samples being submerged in the water, therefore dampening the radiation reaching the vials. The data showed similar results for all locations implying that no variation exists spatially across the lake.

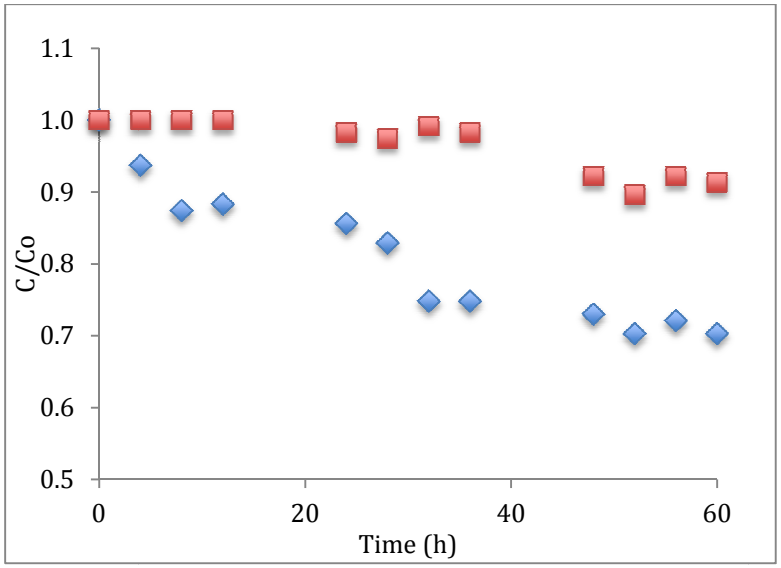

Figure 30. Graph showing the light (blue) and dark (red) samples compared to initial values in location #1 after the second Lake Thoreau three-day experiment.

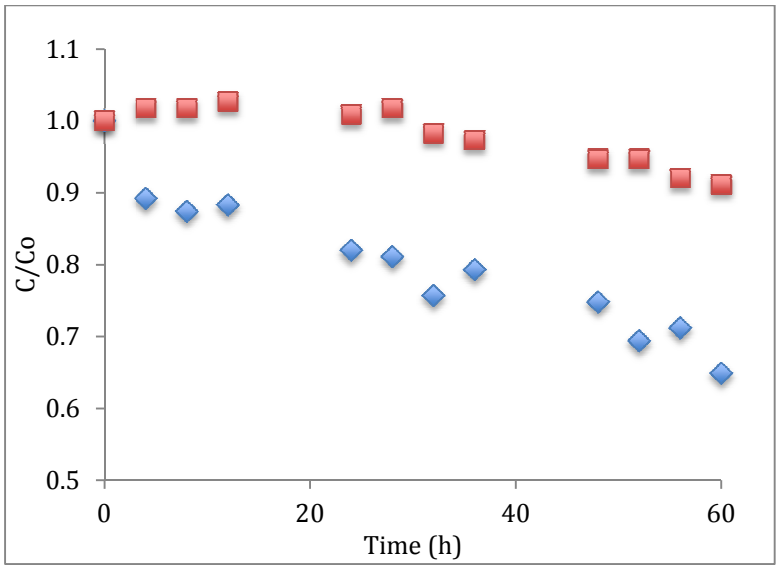

Figure 31. Graph showing the light (blue) and dark (red) samples compared to initial values in location #2 after the second Lake Thoreau three-day experiment.

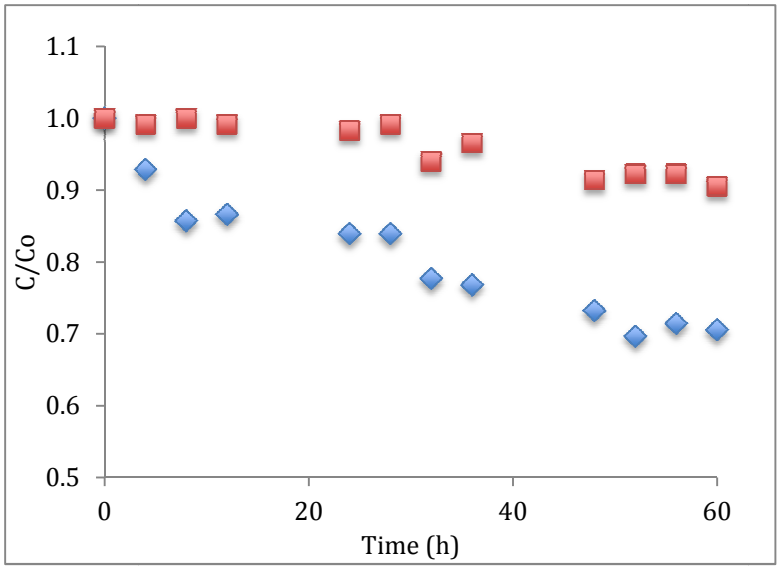

Figure 32. Graph showing the light (blue) and dark (red) samples compared to initial values in location #3 after the second Lake Thoreau three-day experiment.

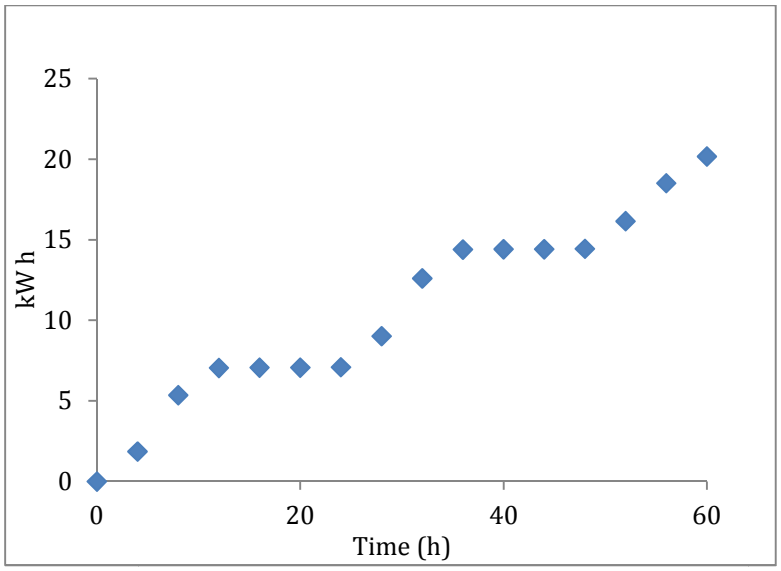

Figure 33. Graph showing the three-day total of irradiance during the second Lake Thoreau test.

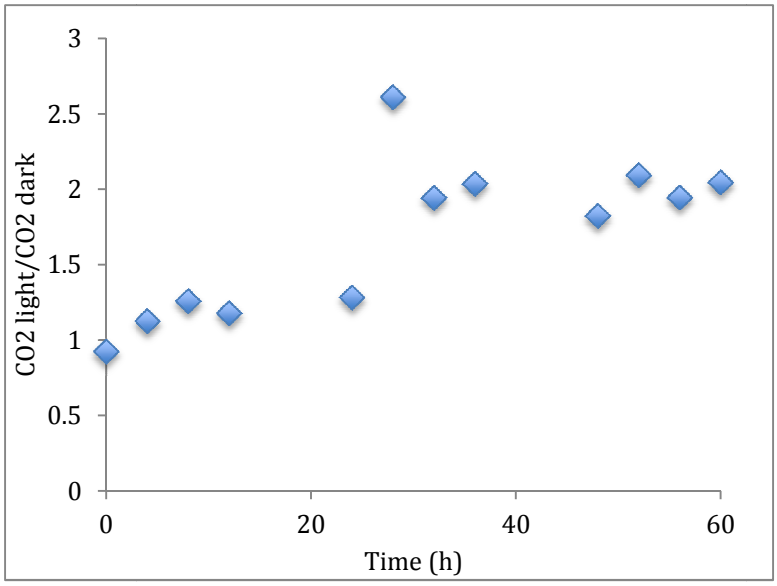

Figure 34. Graph showing the light versus the dark values for CO_2 after the second Lake Thoreau three-day experiment at location #1.

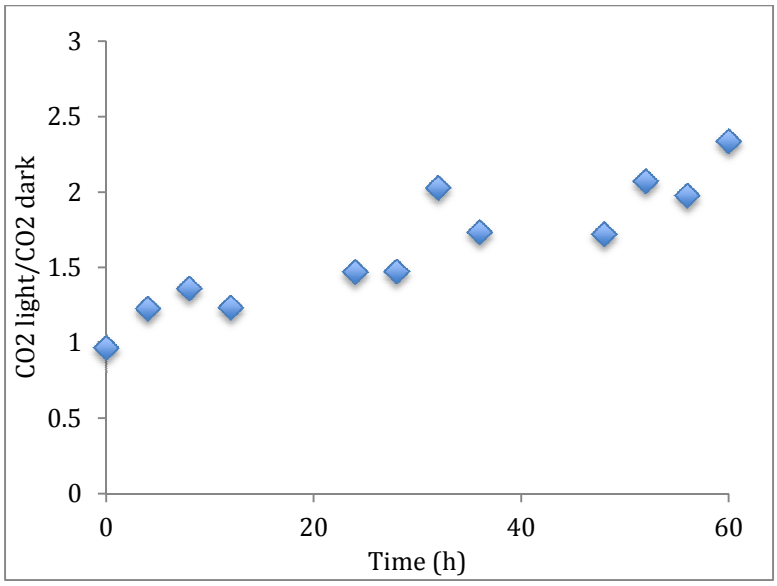

Figure 35. Graph showing the light versus the dark values for CO_2 after the second Lake Thoreau three-day experiment at location #2.

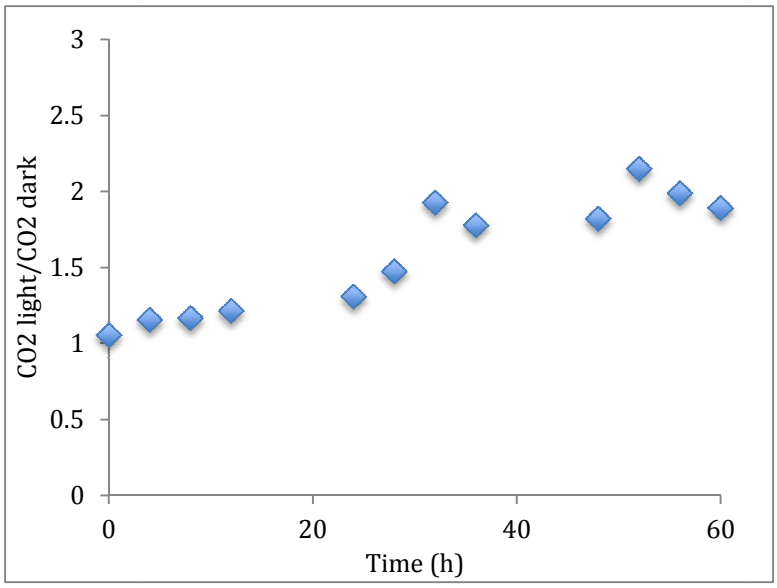

Figure 36. Graph showing the light versus the dark values for CO_2 after the second Lake Thoreau three-day experiment at location #3.

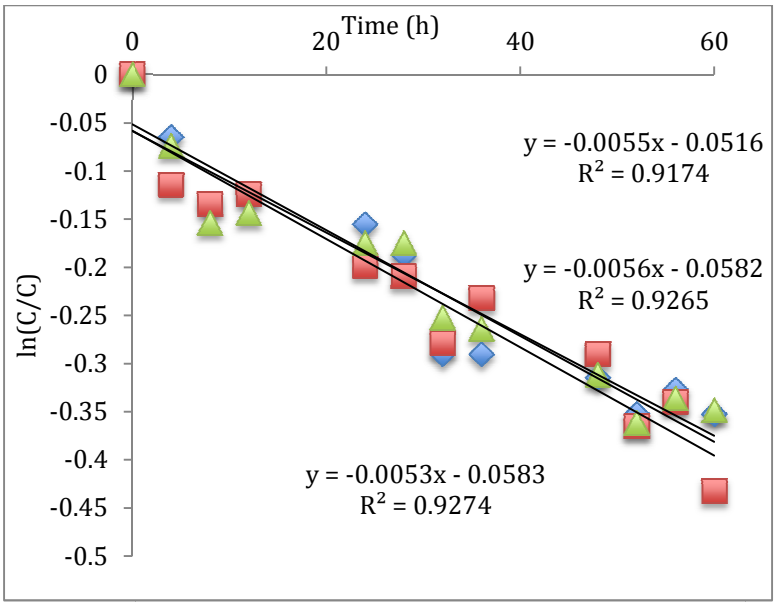

Figure 37. . Graph showing the first order kinetics from the second Lake Thoreau test including location #1 (blue), location #2 (red), and location #3 (green).

CHAPTER VII

ASSESSMENT OF *py*DOC PHOTODEGRADATION AND CO_2 EMISSIONS IN A SALTWATER SYSTEM

Introduction

As the spring rains wash the fresh char from the late winter prescribed burned areas into rivers and into the Gulf of Mexico, the influence of entering the open ocean could have an effect on the photodegradation rates as well as the fate of the degraded *py*DOC. Along with riverine transport, Dittmar et al. (2012) emphasized that tidal fluxed were the primary carriers of *py*DOC in the northern Gulf of Mexico region. To evaluate this, an experiment was designed to focus simply on photodegradation in the Mississippi Sound. To eliminate possible variables and retain the comparison value of the data from this experiment to the Lake Thoreau tests, this experiment is did not involve the addition of a saline stock solution. This experiment focuses on variations in photodegradation rates and the fate of the degraded *py*DOC spatially as the distance from shore varies from nearshore to offshore in the Mississippi Sound. The data from these experiment will then be compared to the results from the experiments at Lake Thoreau and discussed in Chapter VIII

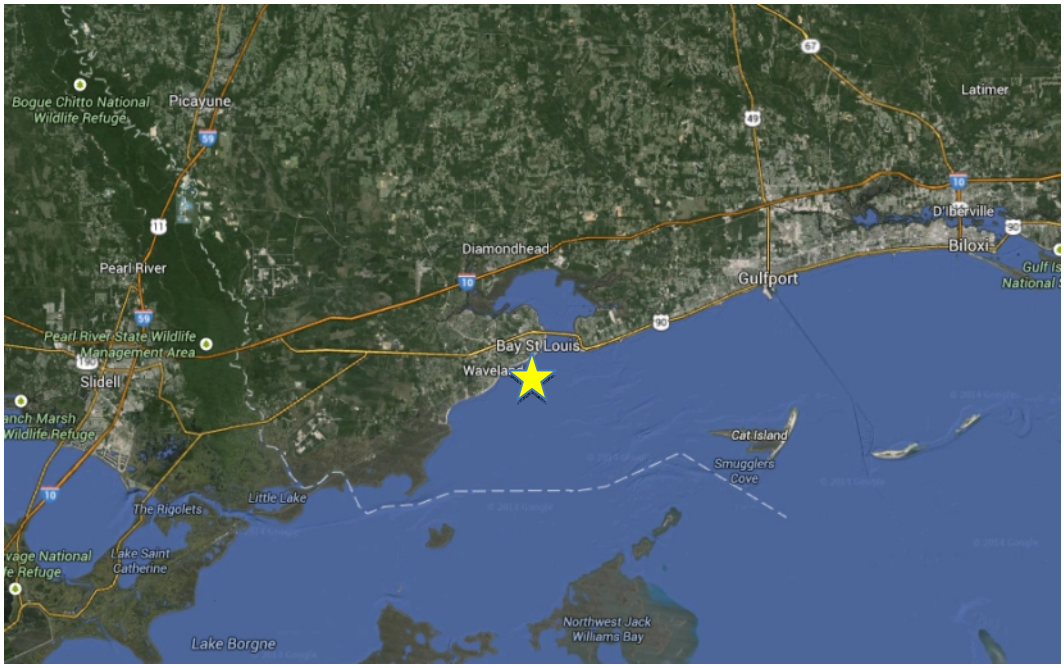

Figure 38. Map showing the location of the experiments in the Mississippi Sound (Google Earth Imagery, 2014).

This experiment utilized the sampling apparatus from the experiments at Lake Thoreau. Samples containing the same non-saline stock solution described in the methods section were attached to the sampling apparati along with control samples wrapped in tin foil. The samples were placed approximately 10, 100, and 300 yards from the shoreline in Waveland, Mississippi. Like the Lake Thoreau experiments, vials were taken from each board for three days at 7am, 11am, 3pm, and 7pm. The samples were collected and brought back to the Hattiesburg campus of The University of Southern Mississippi for analysis. Once in the lab, headspace CO2 was measured by gas chromatography. Then the vials were decrimped and the solution phase analyzed by UV-vis spectrophotometry in absorbance mode (λ_{abs} = 365 nm). The results were then compared to the irradiance levels over the three days. Two three-day experiments were run to ensure consistent results.

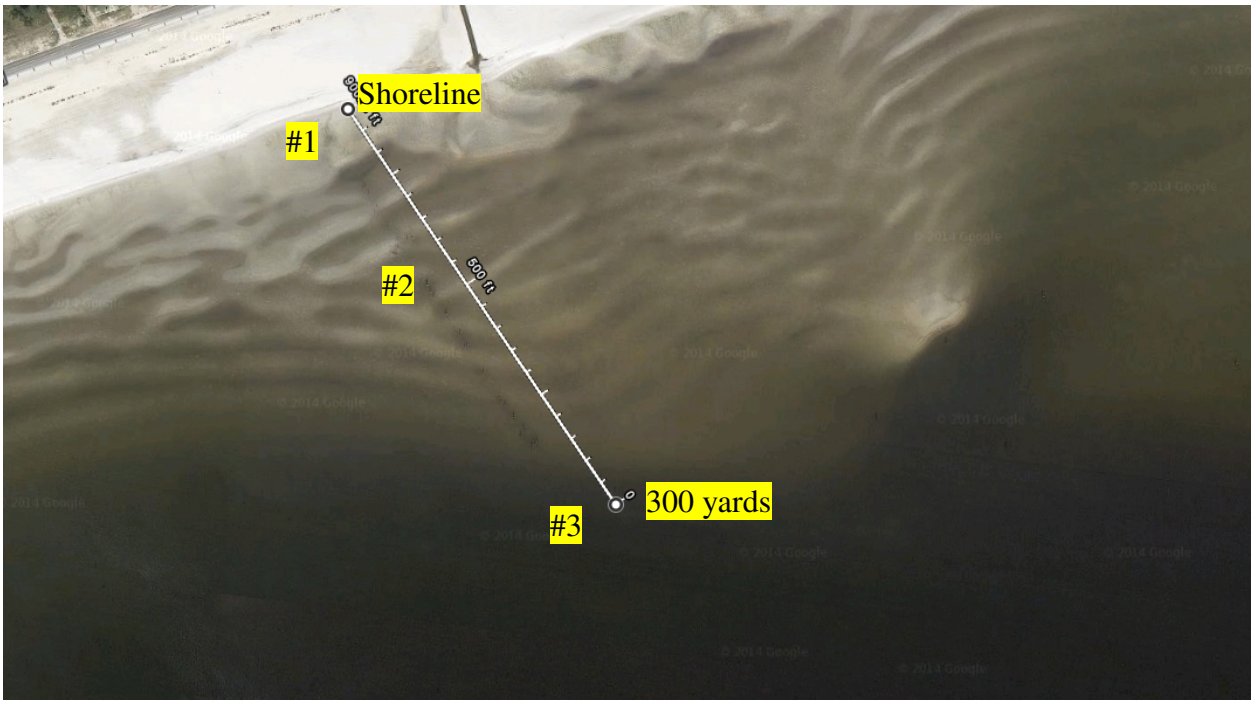

Figure 39. Aerial image showing the area of the three locations used during testing (Google Earth Imagery, 2014).

Experiment #1 Results and Discussion

Data for solar irradiance are integrated values corresponding to the total exposure time up to a given *py*DOC sampling interval. For example, sampling for *py*DOC in these experiments occurred every four hours for sixty hours (three days) hence solar irradiance at 60 h indicate total solar irradiance to which the samples were exposed. At each sampling interval, absorbance was measured, values converted to *py*DOC concentration and presented as C/C_o versus time, where C is the *py*DOC concentration at a given sampling time, t and C_o is the initial *py*DOC at time 0. Total solar irradiance for Day 1, Day 2, and Day 3 were 6.22, 1.40, and 6.93 kW h/m^2, respectively. Except for day two, which experienced extreme cloudiness, the values were consistent with expected ranges for solar irradiation intensity across the NGOM within a given year (Figure 2 and 3). The decline in C/C_o with time and solar irradiance, for light samples on a given test day were

indicative of *py*DOC photodegradation. An increase of around 12% in C/C_o in dark controls indicated no photodegradation and suggested possible contamination resulting in the apparent increase in *py*DOC.

Both quantity and rate of *py*DOC photodegradation were affected by radiation intensity. Approximately 6.1% of pyDOC was photodegraded over a 60 h period when total solar irradiance was 14.55 kW h/m^2, respectively. With storms during the second day of testing much of the data was lost, but some trends were still observable with much lower degradation rates to go along with lower irradiance values as well as not much increase in degradation on day three of the experiment.

Carbon dioxide data for the first Mississippi Sound experiment showed almost five times more headspace CO_2 than the control samples at location one. Location two showed an increase of twice as much CO_2 as its corresponding control after just one day. But unfortunately the second two days of samples were lost. Location three showed an increase of 3.2 times more CO_2 then the control. A steady increase in CO_2 production led to around twice as much CO_2 in the samples in all locations after three days of exposure.

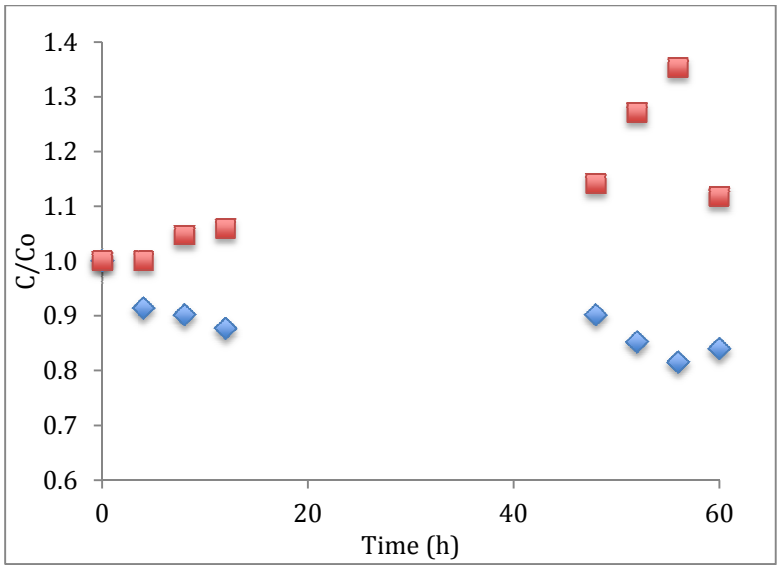

Figure 40. Graph showing the light (blue) and dark (red) samples compared to initial values in location #1 after the first Mississippi Sound three-day experiment.

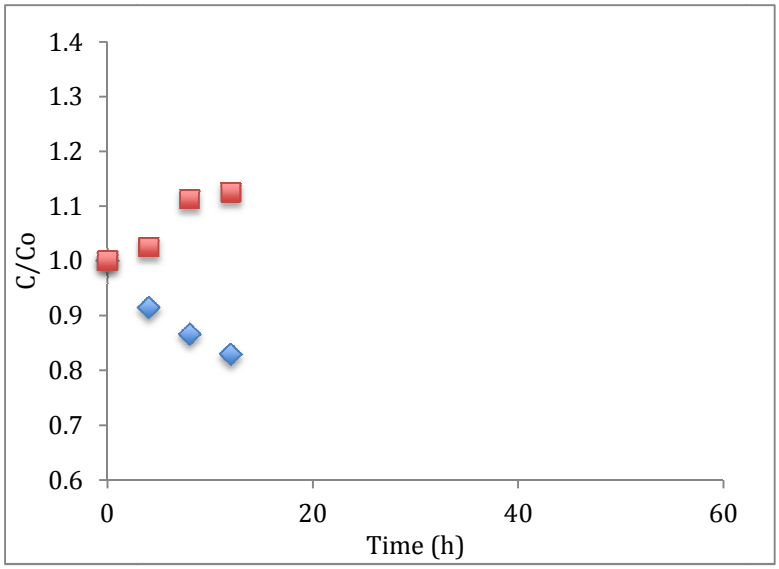

Figure 41. Graph showing the light (blue) and dark (red) samples compared to initial values in location #2 after the first Mississippi Sound three-day experiment.

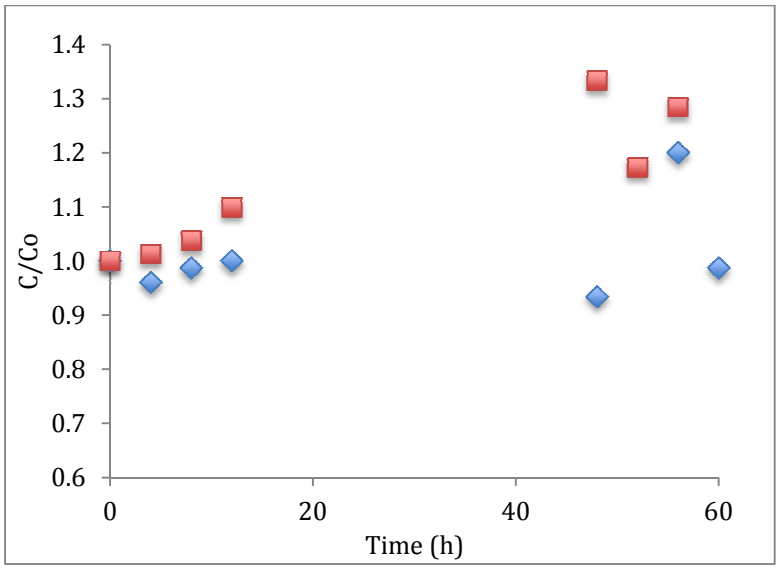

Figure 42. Graph showing the light (blue) and dark (red) samples compared to initial values in location #3 after the first Mississippi Sound three-day experiment.

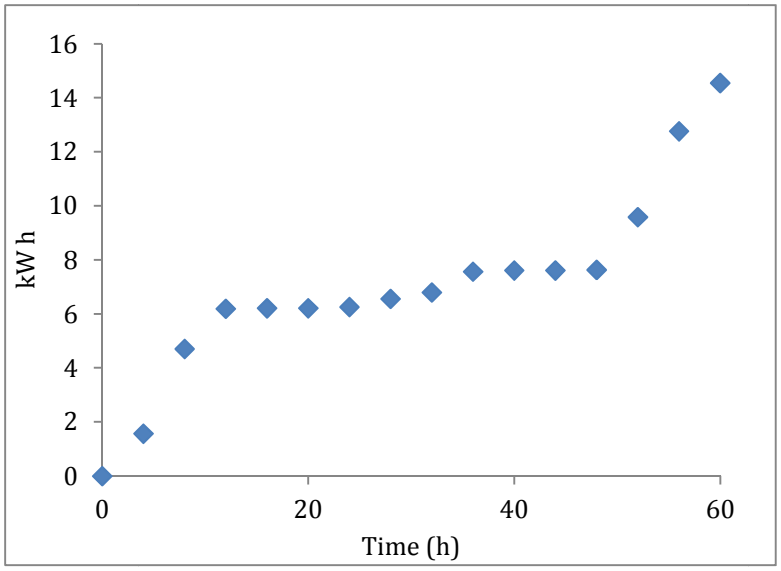

Figure 43. Graph showing the three-day total of irradiance during the first Mississippi Sound test.

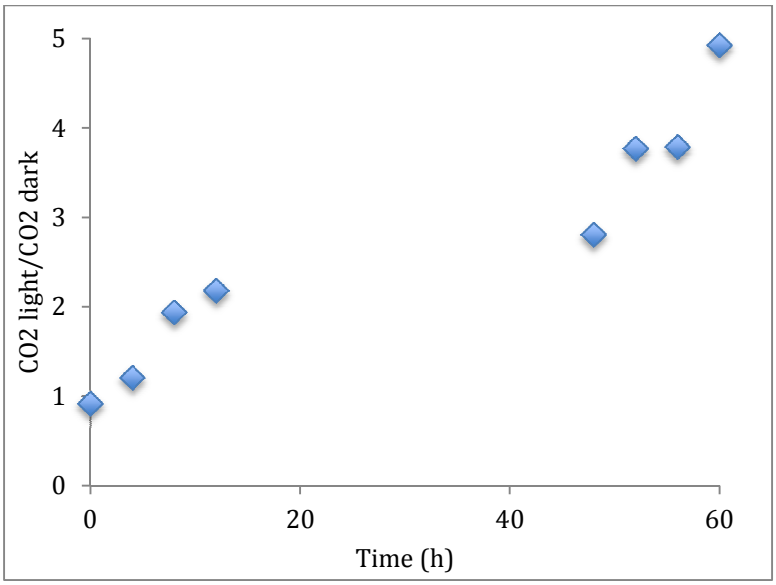

Figure 44. Graph showing the light versus the dark values for CO_2 after the first Mississippi Sound three-day experiment at location #1.

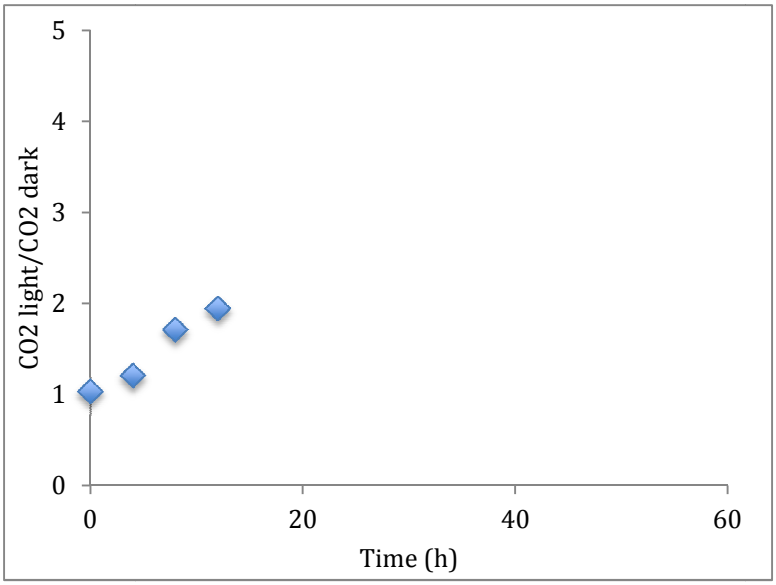

Figure 45. Graph showing the light versus the dark values for CO_2 after the first Mississippi Sound three-day experiment at location #2.

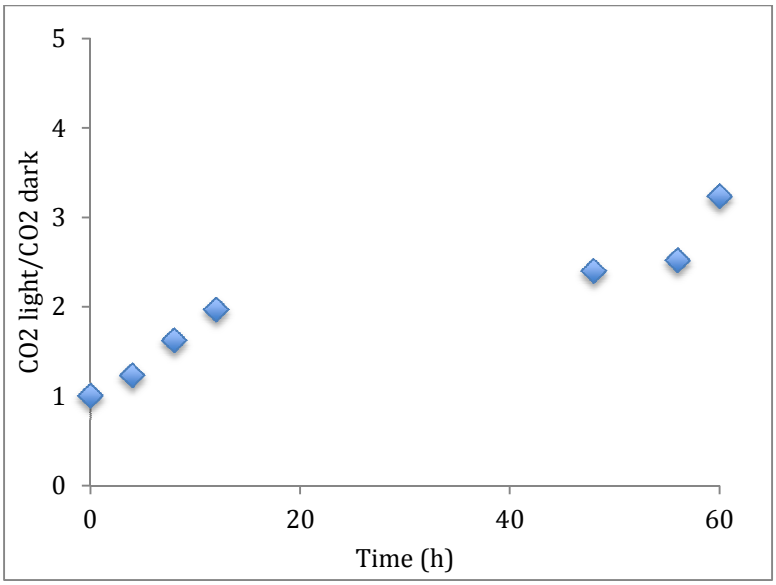

Figure 46. Graph showing the light versus the dark values for CO_2 after the first Mississippi Sound three-day experiment at location #3.

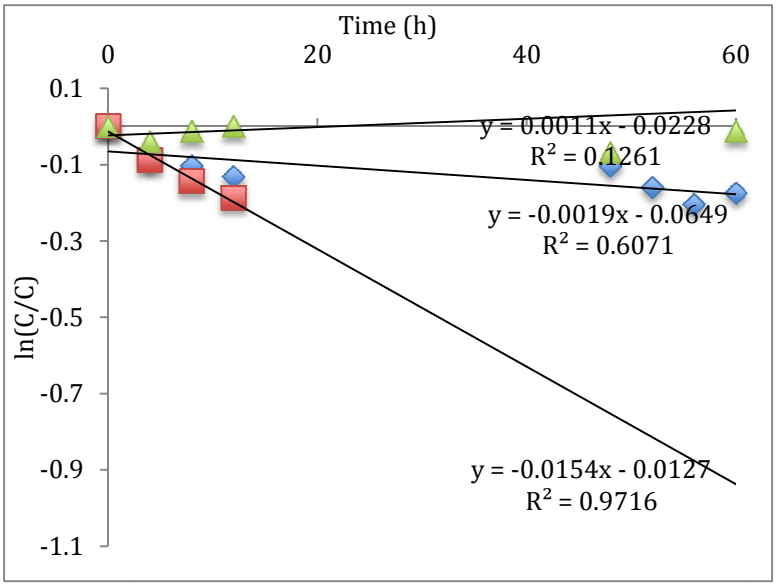

Figure 47. Graph showing the first order kinetics from the first Mississippi Sound test including location #1 (blue), location #2 (green), and location #3 (blue).

Experiment #2 Results and Discussion

Sampling for *py*DOC in this experiment again occurred every four hours for sixty hours (three days) hence solar irradiance at 60 h indicate total solar irradiance to which the samples were exposed. At each sampling interval, absorbance was measured, values converted to *py*DOC concentration and presented as C/C_o versus time, where C is the *py*DOC concentration at a given sampling time, t and C_o is the initial *py*DOC at time, 0. Total solar irradiance for Day 1, Day 2, and Day 3 were 6.57, 4.13, and 7.24 kW h/m^2, respectively. These values were again consistent with expected ranges for solar irradiation intensity across the NGOM within a given year (Figure 2 and 3). The decline in C/C_o with time and solar irradiance, for light samples on a given test day were indicative of *py*DOC photodegradation. An increase in C/C_o in dark controls is consistent with the first experiment in the Mississippi Sound and represents no degradation. The steady increase in *py*DOC of between 20-30% was likely due to contamination or microbial growth throughout the three day experiment.

Both quantity and rate of *py*DOC photodegradation was affected by radiation intensity. Approximately 40, 33, and 40% of pyDOC was photodegraded at the three different locations over a 60 h period when total solar irradiance was 17.94 kW h/m^2, respectively. Not much variation in degradation between the locations was shown in the data and was not expected as in the Lake Thoreau results because all of the samples were getting the same amount of sun in the morning and evening. Loss of pyDOC was relatively continuous on days one and two, but increased severely on day three with results showing around 20% loss of *py*DOC in all locations. This extreme loss on day three being due to the highest single day of irradiance of any experiment run at 7.24 kW h/m^2.

Carbon dioxide data for the second Mississippi Sound experiment showed similar results at all locations. A steady increase in CO_2 production during daylight hours led to around 3.5 times as much CO_2 in samples one and three and four times more in sample two. All locations showed little increase on day two with an irradiance of 4.13 kW h/m^2 and a large increase in headspace CO_2 on day three with an irradiance of 7.24 kW h/m^2.

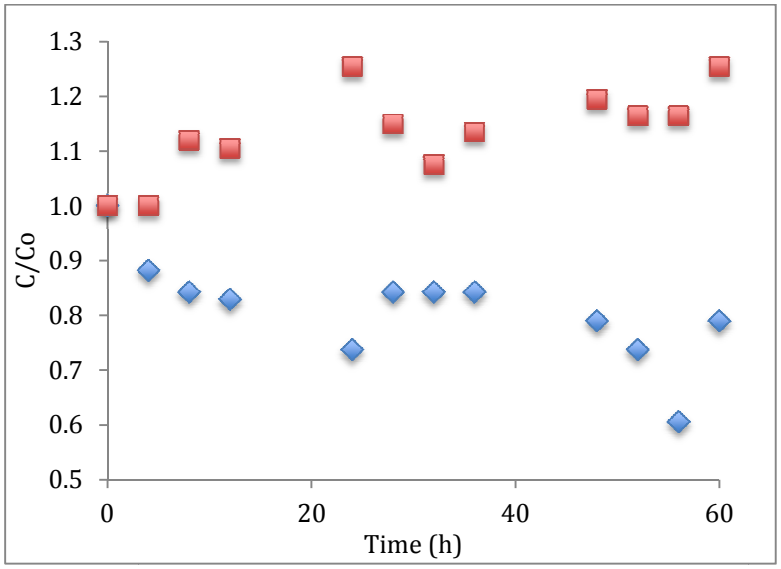

Figure 48. Graph showing the light (blue) and dark (red) samples compared to initial values in location #1 after the second Mississippi Sound three-day experiment.

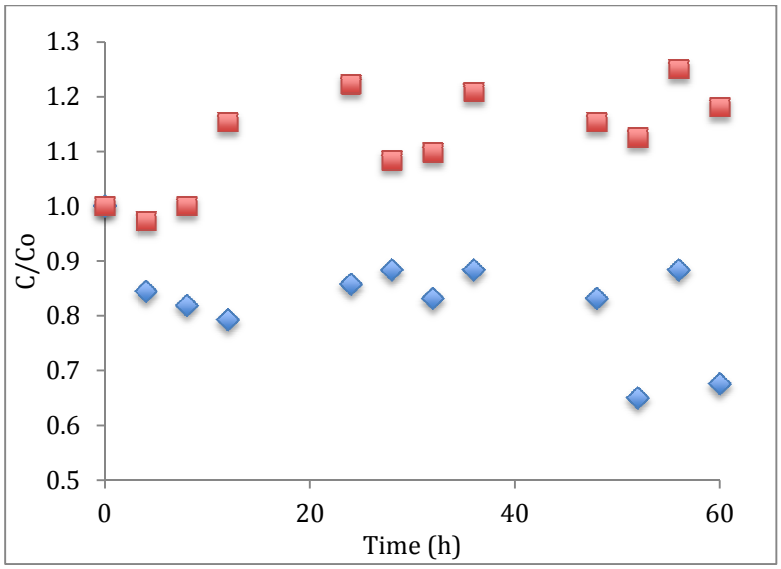

Figure 49. Graph showing the light (blue) and dark (red) samples compared to initial values in location #2 after the second Mississippi Sound three-day experiment.

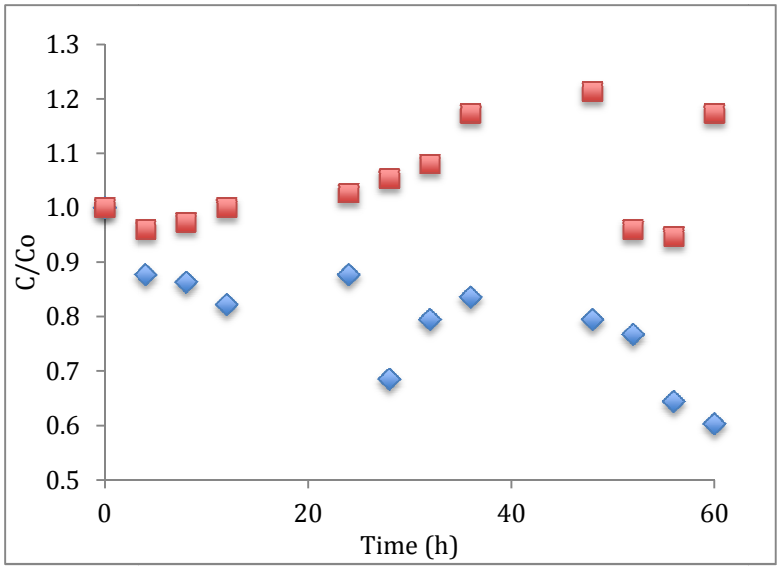

Figure 50. Graph showing the light (blue) and dark (red) samples compared to initial values in location #3 after the second Mississippi Sound three-day experiment.

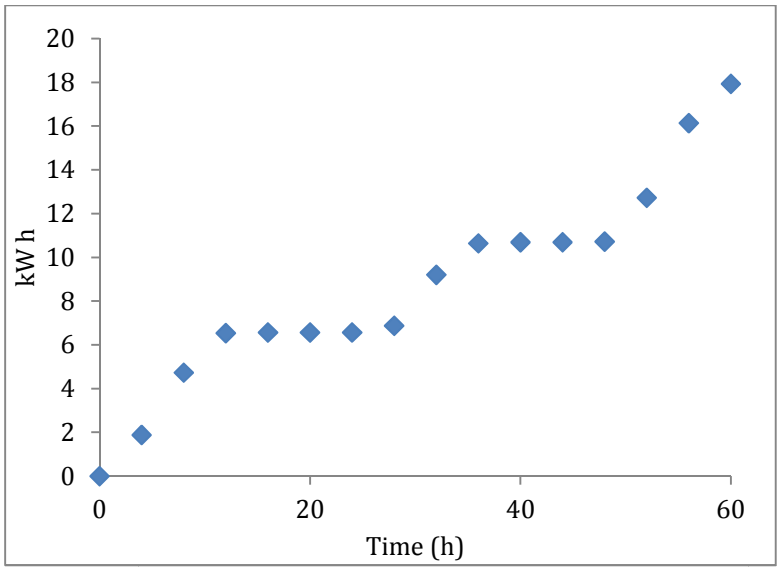

Figure 51. Graph showing the three-day total of irradiance during the second Mississippi Sound test.

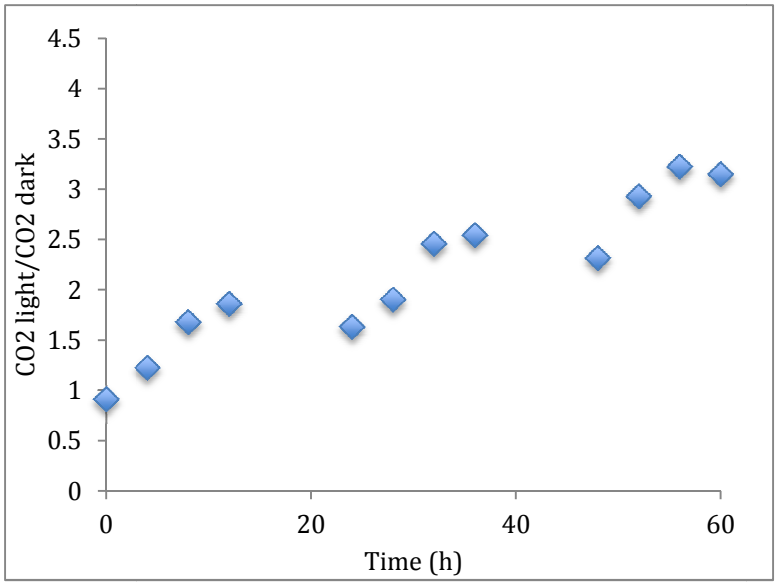

Figure 52. Graph showing the light versus the dark values for CO_2 after the second Mississippi Sound three-day experiment at location #1.

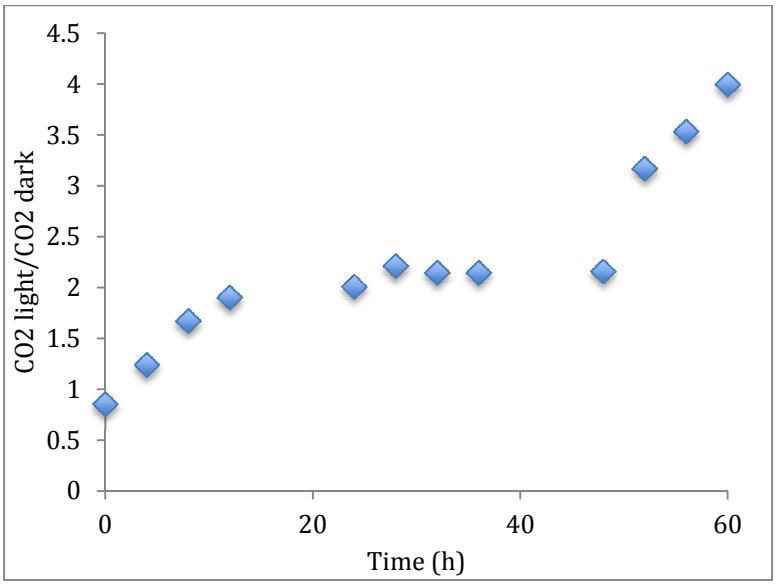

Figure 53. Graph showing the light versus the dark values for CO_2 after the second Mississippi Sound three-day experiment at location #2.

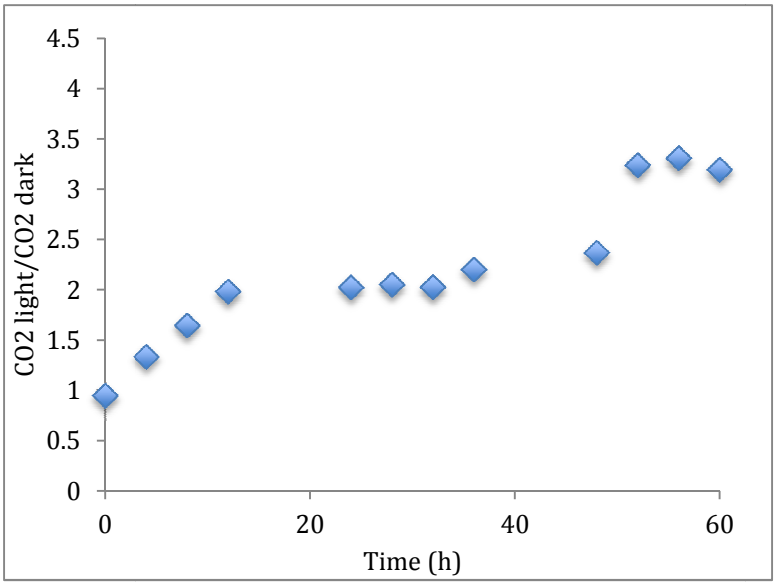

Figure 54. Graph showing the light versus the dark values for CO_2 after the second Mississippi Sound three-day experiment at location #3.

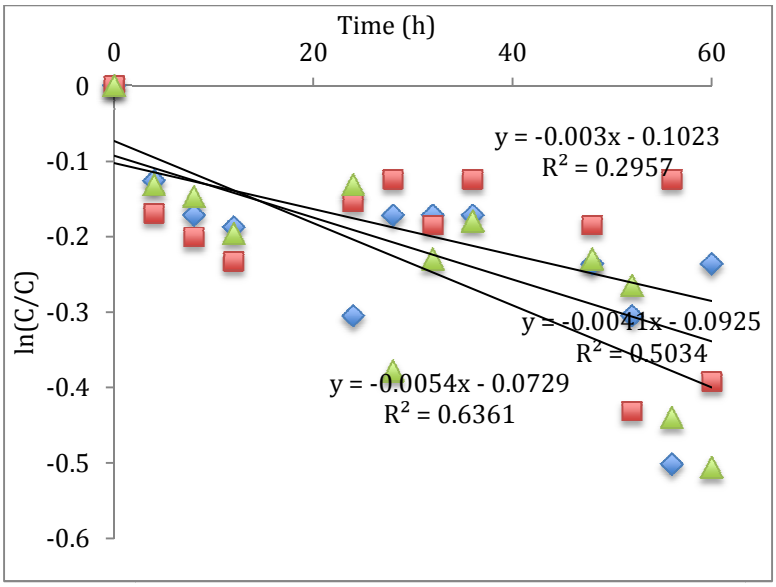

Figure 55. Graph showing the first order kinetics from the second Mississippi Sound test including location #1 (blue), location #2 (red), and location #3 (green).

CHAPTER VIII

CONCLUSIONS

The photodegradation of *py*DOC and associated evolution of CO_2 were studied in exploratory laboratory experiments and various field settings. Experiments were designed to test 1) the effect of solar irradiance on *py*DOC degradation rate, 2) the effect of salinity on photodegradation rate, 3) the effect of irradiance on CO_2 emissions from photodegradation, and 4) the effect of depth on photodegradation. Results from these experiments showed that when exposing samples above the water at the Lake Thoreau weather station, samples lost more than 50% of their PyDOC after just ten hours of exposure. First-order kinetic analysis suggested a photodegradation half-life for *py*DOC of between 9 and 13 hours (0.36-0.54 days) when solar irradiance was between 2.7 and 5.4 kW h/m^2. This was much faster than the estimated half-life of .00136% per day for microbial degradation (Norwood et al., 2013) of *py*DOC and hence suggests that, compared to microbial degradation, photodegradation may have a greater impact on the fate of *py*DOC in subtropical aquatic systems of the NGOM (Kuzyakov, 2009). When samples are exposed below the water surface for three-days, they were found to have lost 12% on average during an experiment with a total of 16 kW h/m^2. The samples showed no significant pattern of *py*DOC loss with distance from the shore. And when the total irradiance a three-day experiment increased to 20 kW h/m^2, the samples lost 31% of their *py*DOC on average. Therefore an increase in irradiance of just 2 kW h/m^2 yielded a 19% increase in degradation. The samples also showed no pattern of *py*DOC loss across the lake. During the first three-day experiment in the Mississippi Sound, samples placed just below the surface of the water were found to have lost around 16% of their *py*DOC during an experiment with a total of 14.5 kW h/m^2. These results came from location one

only because of locations two and three being compromised during a storm. During the second three-day experiment in the Mississippi Sound, samples were found to have lost around 32% of their *py*DOC during an experiment with a total of 18 kW h/m^2. These results were very similar to the Lake Thoreau experiments as increase in irradiance of just 3.5 kW h/m^2 yielded a 16% increase in degradation. The results did indicate a pattern of increasing degradation from location one to location three (nearshore to offshore) in the second experiment in the Mississippi Sound. This variation is likely due to the samples in location one being close to the swash zone where water clarity of the water is much lower than the samples further from shore. As water clarity increases offshore loss of *py*DOC will also be predicted to increase. The rate of *py*DOC loss at varying depths below the surface of the water varied greatly with a 14.1% loss at three inches, 10.3% loss at six inches, and 5.9% loss at twelve inches after twelve and a half hours of exposure. A graph with an exponential trendline (Figure 15) allows the prediction the loss of *py*DOC at a given depth, with the limit of substantial abiotic *py*DOC degradation at around two feet.

An essential lacking point of knowledge in literature is byproducts of photodegraded *py*DOC. By testing the gas chemistry of the headspace of many of the samples, I was able to provide conclusion about the production of CO_2 during photodegradation. During the second Lake Thoreau experiment, samples on average showed around 2.75 times as much CO_2 after three days of exposure than the corresponding control samples. The results did not show any patterns or variations at the different locations throughout the lake. Results from the first Mississippi Sound three-day experiment showed an increase to almost 5 times more CO_2 than the corresponding control samples. The second three-day experiment in the Mississippi Sound showed an

average of around 3.5 times more CO_2 than the control samples with little to no variation in locations.

Although this study breaches knowledge gaps in pyrogenic carbon research, with more than seventy percent of the earth's surface covered in water and the potential for an unknown source of carbon dioxide, the photodegradation of dissolved carbon in this water must be studied in more detail. My hope is that this study will lead to future ones combining both pyrogenic carbon and photodegradation.

REFERENCES

Amon, R., & Benner, R. (1996). Bacterial utilization of different size classes of dissolved organic matter. *Limnology and Oceanography*, *41*(1), 41-51.

Concentrating Solar Resource: Direct Normal [online image]. (2003). Retrieved June 5, 2014 from http://www.nrel.gov/gis/solar.html

Cory, R. M., Crump, B. C., Dobkowski, J. A., & Kling, G. W. (2013). Surface exposure to sunlight stimulates CO_2 release from permafrost soil carbon in the arctic. *National Academy of Sciences of the United States of America*, *119*(9), 3429-3434.

Cory, R. M., Ward, C.P., Crump, B. C., & Kling, G. W. (2014). Sunlight controls water column processing of carbon in arctic fresh waters. *Science, 345*, 925-928.

Cory, R. M., McKnight, D. M., Chin, Y., Miller, P., & Jaros, C. L. (2007). Chemical characteristics of fulvic acids from Arctic surface waters: Microbial contributions and photochemical transformations. *Journal of Geophysical Research*, *112*, 1-14.

Cusack, D. F., Chadwick, O. A., Hockaday, W. C., & Vitousek, P. M. (2012). Mineralogical controls on soil black carbon preservation. *Global Biogeochemical Cycles*, *26*, 1-10.

Dittmar, T., Paeng, J., Gihring, T. M., Suryaputra, I., & Huettel, M. (2012). Discharge of Dissolved Black Carbon from a Fire-Affected Intertidal System. *Limnology and Oceanography*, *57*(4), 1171-1181.

Google Earth Satellite Imagery. (2014).

Graneli, W., Lindell, M., & Tranvik, L. (1996). Photo-oxidative production of dissolved inorganic carbon in lakes of different humic content. *Limnology and Oceanography*, *41*(4), 698-706.

Hedges, J.I., Keil R. G., & Benner R. (1997). What happens to terrestrial organic matter in the ocean? *Organic Geochemistry*, *27*, 195-212.

Jaffé, R., Ding, Y., Niggemann, J., Vahatalo, A., Stubbins, A., Spencer, R., & Campbell, J., Dittmar, T. (2013). Global Charcoal Mobilization from Soils via Dissolution and Riverine Transport to the Oceans. Science, *340*, 345-347.

Jonasson, S., Michelsen A., & Schmidt I. K. (1999). Coupling of nutrient cycling and carbon dynamics in the Arctic, integration of soil microbial and plant processes. *Applied Soil Ecology*, *11*, 135-146.

Kuhlbusch, T. (1998). Enhanced: Black carbon and the carbon cycle. *Science, 280*, 5371, 1903-1904.

Kuzyakov, Y., Subbotina, I., Chen, H., Bogomolova, I., & Xu, X. (2009). Black carbon decomposition and incorporation into soil microbial biomass estimated by ^{14}C labeling. *Soil Biology and Biochemistry*, *41*(2), 210-219.

Mannino, A., & Harvey, O. R. (2004). Black Carbon in Estuarine and Coastal Ocean Dissolved Organic Carbon. *Limnology and Oceanography*, *49*(3), 735-740.

Masiello, C.A., & Louchouarn, P. (2013). Fire in the Ocean. *Science*, *340*(287), 287-288.

Masiello, C.A. (2004). New Directions in Black Carbon Organic Geochemistry. *Marine Chemistry*, *92*, 201-213.

Masiello, C.A., & Druffel, R. M. (1998). Black Carbon in Deep-Sea Sediments. *Science*, *280*, 1911-1913.

Middelburg, J. J., Nieuwenhuize, J., & Breugel, P. (1999). Black Carbon in Marine Sediments. *Marine Chemistry*, *65*, 245-252.

Mitra, S., Bianchi, T. S., Mckee, B.A., & Sutula, M. (2002). Black Carbon from the Mississippi River: Quantities, Sources, and Potential Implications for the Global Carbon Cycle. *Environmental Science Technology*, *36*, 2296-2302.

Moran, M.A., Sheldon Jr., W.M., & Zepp, R.G. (2000). Carbon loss and optical property changes during long-term photochemical and biological degradation of estuarine dissolved organic matter. *Limnology and Oceanography*, *45*(6), 1254-1264.

Norwood, M. J., Louchouam, P., Kuo, L.J., & Harvey, O,R. (2013). Characterization and biodegradation of water-soluble biomarkers and organic carbon extracted from low temperature chars. *Organic Geochemistry, 56*, 111-119.

Shiller, A.M., Duan, S., van Erp, P., & Bianchi, T.S. (2006). Photo-oxidation of dissolved organic matter in river water and its effect on trace element speciation. *Limnology and Oceanography, 51*(4), 1716-1728.

Shrestha, G., Traina, S.J., & Swanston, C.W. (2010). Black Carbon's Properties and Role in the Environment: A Comprehensive Review. *Sustainability, 2*, 294-320.

Simpson, M. J., & Hatcher, P.G. (2004). Overestimates of black carbon in soils and sediments. *Naturwissenschaften*, *91*, 436-440.

Suhett, A. L., Amedo, A.M., Enrich-Prast, A., Esteves, F., & Farjalla, V. (2007). Seasonal changes of dissolved organic carbon photo-oxidation rates in tropical humic lagoon: the role of rainfall as a major regulator. *Science, 64*, 1266-1272.